A High Order Compact Scheme
for the Pure-Streamfunction Formulation
of the Navier-Stokes Equations

M. Ben-Artzi · J.-P. Croisille · D. Fishelov

Abstract In this paper we continue the study, which was initiated in (Ben-Artzi et al. in Math. Model. Numer. Anal. 35(2):313–303, 2001; Fishelov et al. in Lecture Notes in Computer Science, vol. 2667, pp. 809–817, 2003; Ben-Artzi et al. in J. Comput. Phys. 205(2):640–664, 2005 and SIAM J. Numer. Anal. 44(5):1997–2024, 2006) of the numerical resolution of the pure streamfunction formulation of the time-dependent two-dimensional Navier-Stokes equation. Here we focus on enhancing our second-order scheme, introduced in the last three afore-mentioned articles, to fourth order accuracy. We construct fourth order approximations for the Laplacian, the biharmonic and the nonlinear convective operators. The scheme is compact (nine-point stencil) for the Laplacian and the biharmonic operators, which are both treated implicitly in the time-stepping scheme. The approximation of the convective term is compact in the no-leak boundary conditions case and is nearly compact (thirteen points stencil) in the case of general boundary conditions. However, we stress that in any case no unphysical boundary condition was applied to our scheme. Numerical results demonstrate that the fourth order accuracy is actually obtained for several test-cases.

Keywords Navier-Stokes equations · Streamfunction formulation · Vorticity · Numerical algorithm · Compact schemes

M. Ben-Artzi
Institute of Mathematics, The Hebrew University, Jerusalem 91904, Israel
e-mail: mbartzi@math.huji.ac.il

J.-P. Croisille
Department of Mathematics, LMAM, UMR 7122, University of Paul Verlaine-Metz, Metz 57045, France
e-mail: croisil@poncelet.univ-metz.fr

D. Fishelov (✉)
Afeka, Tel-Aviv Academic College of Engineering, 218 Bnei-Efraim St., Tel-Aviv 69107, Israel
e-mail: daliaf@post.tau.ac.il

1 Introduction

The numerical resolution of the classical Navier-Stokes system, governing viscous, incompressible, time-dependent flow, has been an outstanding challenge of computational fluid dynamics since its early stages. The most extensively used approach was the "finite element" method. We do not cite here any references for that topic, not only because the existing literature is so vast, but also because our study here falls into the category of *finite difference* methods. In this category one can find some well-known methods such as "projection methods" ([5, 12, 21, 36, 52] and the references therein), "Spectral methods" [11, 16, 37], "Galerkin methods" [44, 54] and a variety of "velocity-vorticity" [22–24] or "vorticity-streamfunction" methods [25, 26, 46, 47, 53]. See [33, 45] for a review on fundamental formulations of incompressible Navier-Stokes equations. The appearance and growing popularity of "compact schemes" brought a renewed interest in the aforementioned methods [1, 13, 17–19, 27, 35, 42, 43, 50]. The pure-streamfunction formulation for the time-dependent Navier-Stokes system in planar domains has been used in [30–32] some twenty years ago. It has been designed primarily for the numerical investigation of the Hopf bifurcation occurring in the driven cavity problem. Their approach was based on a finite-difference method. The application of various compact schemes to the pure streamfunction formulation is fairly recent [6, 15, 28, 38, 41]. We mention also [20, 34, 39, 40, 48] for works on the stationary Stokes or Navier-Stokes equation. In [7, 8] a comprehensive treatment of a second order compact scheme in space and time is presented. It is based on the Stephenson scheme for the biharmonic problem [50] and includes a detailed analysis of the (linearized) stability and a proof of the convergence of the *fully nonlinear* scheme. In addition, a fast solver for the fourth order elliptic problems, which is applied at each time step, is presented in [9]. We note also that a compact finite-difference (second-order) scheme, based on the same approach, for irregular domains, has recently been presented [10]. Recall that an important feature of the methodology presented in [7, 8] is that the "numerical boundary conditions" are applied only to the streamfunction itself and imposed solely on the boundary. Thus the scheme conforms exactly with the theoretical (pure streamfunction) formulation of the Navier-Stokes system. In particular, this approach avoids:

- Artificial boundary conditions (such as vorticity boundary values).
- Ghost points which are added to the computational domain (in order to improve accuracy).

The main purpose of the present paper is to extend the aforementioned second order scheme [7], to a *fourth order scheme*. With this added accuracy, we are able to simulate the dynamics of flow problems in rectangles with sparser grids and fewer time steps, compared with the second order scheme.

The outline of the paper is as follows. In Sect. 3, we present fourth order approximations for all spatial operators appearing in the evolution equation, i.e., the Laplacian, the biharmonic operator and the nonlinear convective term. Two alternative fourth-order schemes are constructed; the first for "no-leak" or periodic boundary conditions and the second for general boundary conditions.

In Sect. 4 the scheme is coupled with two types of time-stepping schemes. The first is a second order time-stepping scheme, already used in [7]. The second is formally almost third order accurate and was introduced in [49] in the context of Navier-Stokes simulations using spectral methods for the discretization in space.

A detailed analysis of the linear stability properties of the full discrete scheme, is given in Sect. 5.

Finally, in Sect. 6 we present several numerical results, which demonstrate the gain obtained by the increased accuracy.

2 Basic Discrete Operations

For simplicity, assume that $\Omega = [a, b]^2$ is a square. We lay out a uniform grid $a = x_0 < x_1 < \cdots < x_N = b$, $a = y_0 < y_1 < \cdots < y_N = b$. Assume that $\Delta x = \Delta y = h$. At each grid point (x_i, y_j) we have three unknowns $\psi_{i,j}, p_{i,j}, q_{i,j}$, where $p = \psi_x$ and $q = \psi_y$. The connections between ψ and (ψ_x, ψ_y) is the Hermitian relation that we recall below. Let us summarize first some notation for finite difference operators. We assume that the function ψ is regular.

- The centered difference operators $\delta_x \psi$, $\delta_y \psi$, $\delta_x^2 \psi$, $\delta_y^2 \psi$, along with their truncation errors are given by

$$\delta_x \psi_{i,j} = \frac{\psi_{i+1,j} - \psi_{i-1,j}}{2h}, \qquad \delta_x \psi_{i,j} = \partial_x \psi + \frac{1}{6} h^2 \partial_x^3 \psi + O(h^4), \qquad (2.1)$$

$$\delta_y \psi_{i,j} = \frac{\psi_{i,j+1} - \psi_{i,j-1}}{2h}, \qquad \delta_y \psi_{i,j} = \partial_y \psi + \frac{1}{6} h^2 \partial_y^3 \psi + O(h^4), \qquad (2.2)$$

$$\delta_x^2 \psi_{i,j} = \frac{\psi_{i+1,j} - 2\psi_{i,j} + \psi_{i-1,j}}{h^2}, \qquad \delta_x^2 \psi_{i,j} = \partial_x^2 \psi + \frac{1}{12} h^2 \partial_x^4 \psi + O(h^4), \qquad (2.3)$$

$$\delta_y^2 \psi_{i,j} = \frac{\psi_{i,j+1} - 2\psi_{i,j} + \psi_{i,j-1}}{h^2}, \qquad \delta_y^2 \psi_{i,j} = \partial_y^2 \psi + \frac{1}{12} h^2 \partial_y^4 \psi + O(h^4). \qquad (2.4)$$

- The *Hermitian gradient* (ψ_x, ψ_y) is defined by the two relations

$$\begin{cases} \left(I + \frac{h^2}{6} \delta_x^2\right) \psi_{x,i,j} = \delta_x \psi_{i,j}, & 1 \le i, j \le N - 1, \\ \left(I + \frac{h^2}{6} \delta_y^2\right) \psi_{y,i,j} = \delta_y \psi_{i,j}, & 1 \le i, j \le N - 1. \end{cases} \qquad (2.5)$$

The Hermitian gradient (ψ_x, ψ_y) is fourth order accurate in the two directions x and y with a truncation error given by

$$\psi_{x,i,j} = \partial_x \psi - \frac{1}{180} h^4 \partial_x^5 \psi + O(h^6), \qquad (2.6)$$

$$\psi_{y,i,j} = \partial_y \psi - \frac{1}{180} h^4 \partial_y^5 \psi + O(h^6). \qquad (2.7)$$

- The Stephenson one-dimensional fourth-order finite-difference operators are defined at each grid point (x_i, y_j), $1 \le i, j \le N - 1$ by (see [7]),

$$\delta_x^4 \psi_{i,j} = \frac{12}{h^2} \{(\delta_x \psi_x)_{i,j} - \delta_x^2 \psi_{i,j}\}, \qquad \delta_x^4 \psi_{i,j} = \partial_x^4 \psi - \frac{1}{720} h^4 \partial_x^8 \psi + O(h^6), \qquad (2.8)$$

$$\delta_y^4 \psi_{i,j} = \frac{12}{h^2} \{(\delta_y \psi_y)_{i,j} - \delta_y^2 \psi_{i,j}\}, \qquad \delta_y^4 \psi_{i,j} = \partial_y^4 \psi - \frac{1}{720} h^4 \partial_y^8 \psi + O(h^6). \qquad (2.9)$$

Thus, the local truncation errors are of fourth order accuracy.
- The operators δ_x^+ and δ_y^+ are defined by

$$\delta_x^+ \psi_{i,j} = \frac{\psi_{i+1,j} - \psi_{i,j}}{h}, \qquad \delta_y^+ \psi_{i,j} = \frac{\psi_{i,j+1} - \psi_{i,j}}{h} \qquad (2.10)$$

and are clearly first order approximations of $\partial_x \psi$ and $\partial_y \psi$.

- The forward discrete averaging operators μ_x, μ_y are defined by

$$\mu_x \psi_{i,j} = \frac{1}{2}(\psi_{i,j} + \psi_{i+1,j}), \qquad \mu_y \psi_{i,j} = \frac{1}{2}(\psi_{i,j} + \psi_{i,j+1}). \tag{2.11}$$

We consider continuous functions ψ which vanish, along with their gradients, on the boundary. The discrete analogue, which we denote by $L_{0,h}^2 \times (L_{0,h}^2)^2$, consists of grid functions $\psi_{i,j}$, $\psi_{x,i,j}$, $\psi_{y,i,j}$ with zero values at boundary points. We regard the grid-functions $\psi_{i,j}$, $1 \le i, j \le N - 1$, as elements of $\mathbb{R}^{(N-1)^2}$, equipped with the scalar product in $L_{0,h}^2$

$$(\psi, \phi)_h = h^2 \sum_{i,j=1}^{N-1} \psi_{i,j} \phi_{i,j}. \tag{2.12}$$

Whenever needed, boundary values of ψ, ψ_x, ψ_y are taken as zero. Thus, we set, for example, $\delta_x^+ \psi_{0,j} = \frac{\psi_{1,j} - \psi_{0,j}}{2h} = \frac{\psi_{1,j}}{2h}$.

3 Fourth Order Spatial Discretization of the Navier-Stokes Equation

3.1 The Second Order Pure Streamfunction Scheme

In this subsection, we recall briefly the second order pure streamfunction scheme, which is the basis of the present study. We consider the Navier-Stokes equation in pure streamfunction form

$$\begin{cases} \partial_t \Delta \psi + \nabla^\perp \psi \cdot \nabla \Delta \psi - \nu \Delta^2 \psi = f(x, y, t), \\ \psi(x, y, t) = \psi_0(x, y). \end{cases} \tag{3.1}$$

Recall that $\nabla^\perp \psi = (-\partial_y \psi, \partial_x \psi)$ is the velocity vector. Equation (3.1) is rewritten as

$$\partial_t \Delta \psi - \partial_y \psi \Delta \partial_x \psi + \partial_x \psi \Delta \partial_y \psi - \nu \Delta^2 \psi = f(x, y, t). \tag{3.2}$$

The design of the scheme proceeds along the method of lines. This means that we first discretize the equation in space, then in time. The spatial discretization is obtained simply by plugging in (3.2) the following second order approximations:

- The five point discrete Laplacian

$$\Delta_h \psi_{i,j} = \delta_x^2 \psi_{i,j} + \delta_y^2 \psi_{i,j} \tag{3.3}$$

with truncation error

$$\Delta_h \psi_{i,j} = \Delta \psi + \frac{1}{12} h^2 (\partial_x^4 \psi + \partial_y^4 \psi) + O(h^4). \tag{3.4}$$

- The Stephenson second order biharmonic operator

$$\Delta_h^2 \psi_{i,j} = \delta_x^4 \psi_{i,j} + \delta_y^4 \psi_{i,j} + 2\delta_x^2 \delta_y^2 \psi_{i,j} \tag{3.5}$$

with truncation error

$$\Delta_h^2 \psi_{i,j} = \Delta^2 \psi + \frac{1}{6} h^2 (\partial_x^2 \partial_y^4 \psi + \partial_x^4 \partial_y^2 \psi) + O(h^4). \tag{3.6}$$

- The second order discrete convective term $C_h(\psi)$

$$C_h(\psi)_{i,j} = -\psi_{y,i,j}(\Delta_h\psi_x)_{i,j} + \psi_{x,i,j}(\Delta_h\psi_y)_{i,j}. \tag{3.7}$$

At grid point (x_i, y_j) and time t, the semi-discrete second order scheme for the time-dependent Navier-Stokes equation is

$$\frac{d}{dt}\Delta_h\psi_{i,j}(t) + C_h(\psi(t))_{i,j} - \nu\Delta_h^2\psi_{i,j}(t) = f(x_i, y_j, t). \tag{3.8}$$

A second order time-stepping scheme is then used to perform the time integration. This is discussed in more details in Sect. 4 below. Extensive numerical results, stability and convergence analysis for the second order scheme, as well as an efficient fast solver, were carried out in [7–9]. We now turn to the goal of this paper, namely the derivation of a discrete approximation to (3.1), which is fourth-order accurate in the spatial variables.

3.2 Fourth Order Discrete Laplacian and Biharmonic Operators

The fourth order discrete Laplacian $\tilde{\Delta}_h\psi$ and biharmonic $\tilde{\Delta}_h^2\psi$ operators introduced in [9] are perturbations of the second order operators (3.3) and (3.5). This perturbation is based on the explicit truncation error displayed in (3.4) for the Laplacian.

$$\tilde{\Delta}_h\psi = \Delta_h\psi - \frac{h^2}{12}(\delta_x^4 + \delta_y^4)\psi. \tag{3.9}$$

In other words, the expression is clearly a fourth-order approximation of $\Delta\psi$. In fact, using the expressions (2.3), (2.4) for $\delta_x^2\psi$, $\delta_y^2\psi$ and (2.8), (2.9) for $\delta_x^4\psi$, $\delta_y^4\psi$, we can define a fourth order version of the discrete Laplacian as

$$\tilde{\Delta}_h\psi = 2\Delta_h\psi - (\delta_x\psi_x + \delta_y\psi_y). \tag{3.10}$$

We note that the precise fourth-order truncation error is

$$\tilde{\Delta}_h\psi_{i,j} - \Delta\psi = \frac{1}{360}h^4(\partial_x^6\psi + \partial_y^6\psi) + O(h^6). \tag{3.11}$$

Similarly, we define

$$\tilde{\Delta}_h^2\psi = \Delta_h^2\psi - \frac{h^2}{6}(\delta_x^2\delta_y^4 + \delta_x^4\delta_y^2)\psi = \delta_x^4\left(I - \frac{h^2}{6}\delta_y^2\right)\psi + \delta_y^4\left(I - \frac{h^2}{6}\delta_x^2\right)\psi + 2\delta_x^2\delta_y^2\psi. \tag{3.12}$$

The associated truncation error is given by

$$\tilde{\Delta}_h^2\psi_{i,j} - \Delta^2\psi = -h^4\left(\frac{1}{720}(\partial_x^8\psi + \partial_y^8\psi) + \frac{1}{72}\partial_x^4\partial_y^4\psi - \frac{1}{180}(\partial_x^2\partial_y^6\psi + \partial_x^6\partial_y^2\psi)\right) + O(h^6). \tag{3.13}$$

Recall that the second order Laplacian and biharmonic operators are self-adjoint and positive. Assume that $\psi, \phi \in L_{h,0}^2$. Then, for the Laplacian we have

$$-(\Delta_h\psi, \phi)_h = (\delta_x^+\psi, \delta_x^+\phi)_h + (\delta_y^+\psi, \delta_y^+\phi)_h. \tag{3.14}$$

In addition, if (ψ_x, ψ_y), $(\phi_x, \phi_y) \in L_{h,0}^2$ are the Hermitian gradients related to ψ, ϕ by (2.6), (2.7), we have (see [8], (138))

$$(\Delta_h^2 \psi, \phi)_h = (\delta_x^+ \psi_x, \delta_x^+ \phi_x)_h + (\delta_y^+ \psi_y, \delta_y^+ \phi_y)_h + 2(\delta_x^+ \delta_y^+ \psi, \delta_x^+ \delta_y^+ \phi)_h$$

$$+ \frac{12}{h^2}(\delta_x^+ \psi - \mu_x \psi_x, \delta_x^+ \phi - \mu_x \phi_x)_h$$

$$+ \frac{12}{h^2}(\delta_y^+ \psi - \mu_y \psi_y, \delta_y^+ \phi - \mu_y \phi_y)_h. \tag{3.15}$$

The last two equalities form the basis of the stability and convergence analysis for the discrete Laplace and biharmonic equations, where the operators are chosen as Δ_h and Δ_h^2 (see [8]). Similarly, for the fourth order operators $\tilde{\Delta}_h$, $\tilde{\Delta}_h^2$, we have

Proposition 3.1 (Symmetry and coercivity of the operators $-\tilde{\Delta}_h$, $\tilde{\Delta}_h^2$) *If $\psi, \phi \in L_{h,0}^2$ and $(\psi_x, \psi_y), (\phi_x, \phi_y) \in L_{h,0}^2$ are the corresponding Hermitian gradients, then:*

(i) *The fourth order Laplacian $\tilde{\Delta}_h$ satisfies the relation*

$$-(\tilde{\Delta}_h \psi, \phi)_h = (\delta_x^+ \psi, \delta_x^+ \phi)_h + (\delta_y^+ \psi, \delta_y^+ \phi)_h$$

$$+ (\delta_x^+ \psi - \mu_x \psi_x, \delta_x^+ \phi - \mu_x \phi_x)_h + (\delta_y^+ \psi - \mu_y \psi_y, \delta_y^+ \phi - \mu_y \phi_y)_h$$

$$+ \frac{h^2}{12} \left((\delta_x^+ \psi_x, \delta_x^+ \phi_x)_h + (\delta_y^+ \psi_y, \delta_y^+ \phi_y)_h \right).$$

(ii) *The fourth order biharmonic $\tilde{\Delta}_h^2$ satisfies the relation*

$$(\tilde{\Delta}_h^2 \psi, \phi)_h = (\delta_x^+ \psi_x, \delta_x^+ \phi_x)_h + (\delta_y^+ \psi_y, \delta_y^+ \phi_y)_h + 2(\delta_x^+ \delta_y^+ \psi, \delta_x^+ \delta_y^+ \phi)_h$$

$$+ \frac{12}{h^2}(\delta_x^+ \psi - \mu_x \psi_x, \delta_x^+ \phi - \mu_x \phi_x)_h + \frac{12}{h^2}(\delta_y^+ \psi - \mu_y \psi_y, \delta_y^+ \phi - \mu_y \phi_y)_h$$

$$+ \frac{h^2}{6} \left((\delta_x^+ \delta_y^+ \psi_x, \delta_x^+ \delta_y^+ \phi_x)_h + (\delta_x^+ \delta_y^+ \psi_y, \delta_x^+ \delta_y^+ \phi_y)_h \right)$$

$$+ 2(\delta_y^+ (\delta_x^+ \psi - \mu_x \psi_x), \delta_y^+ (\delta_x^+ \phi - \mu_x \phi_x))_h$$

$$+ 2(\delta_x^+ (\delta_y^+ \psi - \mu_y \psi_y), \delta_x^+ (\delta_y^+ \phi - \mu_y \phi_y))_h.$$

Proof Note the following identity (see [8], (88))

$$(\delta_x^4 \psi, \phi)_h = (\delta_x^+ \psi_x, \delta_x^+ \phi_x)_h + \frac{12}{h^2}(\delta_x^+ \psi - \mu_x \psi, \delta_x^+ \phi - \mu_x \phi)_h. \tag{3.16}$$

Combining this equation with (3.9) and (3.14) yields (i). We turn now to part (ii). Consider the two terms $\delta_y^2 \delta_x^4$ and $\delta_x^2 \delta_y^4$ in (3.12). A discrete integration by parts and (3.16) gives

$$(\delta_y^2 \delta_x^4 \psi, \phi)_h = -(\delta_y^+ \delta_x^4 \psi, \delta_y^+ \phi)_h = -(\delta_x^+ \delta_y^+ \psi_x, \delta_x^+ \delta_y^+ \phi_x)_h$$

$$- \frac{12}{h^2}(\delta_x^+ \delta_y^+ \psi - \mu_x \delta_y^+ \psi_x, \delta_x^+ \delta_y^+ \phi - \mu_x \delta_y^+ \phi_x)_h. \tag{3.17}$$

Similarly,

$$(\delta_x^2 \delta_y^4 \psi, \phi)_h = -(\delta_x^+ \delta_y^4 \psi, \delta_x^+ \phi)_h = -(\delta_x^+ \delta_y^+ \psi_y, \delta_x^+ \delta_y^+ \phi_y)_h$$

$$- \frac{12}{h^2}(\delta_x^+ \delta_y^+ \psi - \mu_y \delta_x^+ \psi_y, \delta_x^+ \delta_y^+ \phi - \mu_y \delta_x^+ \phi_y)_h. \tag{3.18}$$

Combining (3.12), (3.15), (3.17) and (3.18) yields the result. $\square$

Corollary 3.1 (Positivity of the operators $-\tilde{\Delta}_h$, $\tilde{\Delta}_h^2$) *If* $\psi, \phi \in L_{h,0}^2$ *and* (ψ_x, ψ_y), *$(\phi_x, \phi_y) \in L_{h,0}^2$ are the corresponding Hermitian gradients, then $-\tilde{\Delta}_h$ and $\tilde{\Delta}_h^2$ are positive and in fact*

$$-(\tilde{\Delta}_h\psi, \psi)_h \geq -(\Delta_h\psi, \psi)_h = |\delta_x^+\psi|_h^2 + |\delta_y^+\psi|_h^2, \tag{3.19}$$

$$(\tilde{\Delta}_h^2\psi, \psi)_h \geq (\Delta_h^2\psi, \psi)_h \geq C(|\delta_x^+\psi_x|_h^2 + |\delta_y^+\psi_y|_h^2 + |\delta_x^+\psi_y|_h^2 + |\delta_y^+\psi_x|_h^2). \tag{3.20}$$

3.3 A Fourth Order Convective Term: No-leak or Periodic Boundary Conditions

The convective term in the Navier-Stokes equation (3.1) is

$$u \cdot \partial_x \Delta\psi + v \cdot \partial_y \Delta\psi = \nabla^\perp\psi \cdot \nabla\Delta\psi = -\partial_y\psi\Delta\partial_x\psi + \partial_x\psi\Delta\partial_y\psi := C(\psi), \tag{3.21}$$

where the velocity $\mathbf{u} = (u, v) = \nabla^\perp\psi$. In this section we present a finite difference operator, which retains the compact stencil of nine points, without any special treatment at near boundary points. It is fourth-order accurate in the specific cases of no-leak or periodic boundary conditions. In the previous work [8] we applied the following finite difference operator to approximate the convective term (3.21).

$$C_h(\psi) = -\psi_y\Delta_h\psi_x + \psi_x\Delta_h\psi_y. \tag{3.22}$$

Note that replacing in (3.22) Δ_h by $\tilde{\Delta}_h$ would formally make this term fourth-order accurate. However, applying $\tilde{\Delta}_h$ to ψ_x forces us (see (3.10)) to use the operator $\delta_x\psi_{xx}$ at near boundary points, hence to use zero boundary values for ψ_{xx}. This is in contradiction to the continuous case, where the vorticity $\Delta\psi$ does not in general vanish on the boundary. It can be shown that the truncation error in (3.22) is

$$C_h(\psi) - C(\psi) = \frac{h^2}{12}\left(-\partial_y\psi\partial_x(\partial_x^4\psi + \partial_y^4\psi) + \partial_x\psi\partial_y(\partial_x^4\psi + \partial_y^4\psi)\right) + O(h^4). \tag{3.23}$$

Since the velocity $(u, v) = (-\partial_y\psi, \partial_x\psi)$ is divergence free, the term in parenthesis in the right-hand side of the last equation can be written in conservative form as follows:

$$-\partial_y\psi\partial_x(\partial_x^4\psi + \partial_y^4\psi) + \partial_x\psi\partial_y(\partial_x^4\psi + \partial_y^4\psi)$$
$$= \partial_x(u(\partial_x^4\psi + \partial_y^4\psi)) + \partial_y(v(\partial_x^4\psi + \partial_y^4\psi))$$
$$= \partial_x(-\partial_y\psi(\partial_x^4\psi + \partial_y^4\psi)) + \partial_y(\partial_x\psi(\partial_x^4\psi + \partial_y^4\psi)).$$

Note that this form is invariant under any coordinate transformation. Replacing the partial derivatives, appearing in the right-hand side of the last equation, by second order accurate finite difference operators yields

$$\partial_x(-\partial_y\psi(\partial_x^4\psi + \partial_y^4\psi)) + \partial_y(\partial_x\psi(\partial_x^4\psi + \partial_y^4\psi))$$
$$= \delta_x(-\psi_y(\delta_x^4\psi + \delta_y^4\psi)) + \delta_y(\psi_x(\delta_x^4\psi + \delta_y^4\psi)) + O(h^2). \tag{3.24}$$

Therefore, fourth order approximation of the convective term $C(\psi)$ in (3.21) may be written (using 3.23) as

$$\tilde{C}_h(\psi) = -\psi_y\Delta_h\psi_x + \psi_x\Delta_h\psi_y - \frac{h^2}{12}\left(\delta_x(-\psi_y(\delta_x^4\psi + \delta_y^4\psi)) + \delta_y(\psi_x(\delta_x^4\psi + \delta_y^4\psi))\right)$$
$$= C(\psi) + O(h^4). \tag{3.25}$$

The difficulty with this expression is that it involves high-order differences, appearing in the term

$$J = \delta_x(-\psi_y(\delta_x^4\psi + \delta_y^4\psi)) + \delta_y(\psi_x(\delta_x^4\psi + \delta_y^4\psi)). \tag{3.26}$$

We show now that in the special case of zero boundary conditions, we can still evaluate J at each interior point, including near-boundary points. Consider the term $\delta_x(-\psi_y(\delta_x^4\psi + \delta_y^4\psi))$ at near boundary points, in particular near the left or right sides of the square. This requires the knowledge of $\delta_x^4\psi$ on the boundary. The latter is known for periodic problems, since in this case all points are interior points. Alternatively, we consider the specific case of no-leak boundary conditions. Along the left and right sides the no-leak condition reads $u = -\psi_y = 0$. Hence, the term $-\psi_y(\delta_x^4\psi + \delta_y^4\psi)$ is zero on the boundary. Thus, $\delta_x(-\psi_y(\delta_x^4\psi + \delta_y^4\psi))$ is computable near left/right sides. Along the top/bottom sides, no problem arises when one computes the value of $\delta_x(-\psi_y(\delta_x^4\psi + \delta_y^4\psi))$ at near-boundary points, since δ_x operates in the x direction only. Similar considerations hold for $\delta_y(-\psi_x(\delta_x^4\psi + \delta_y^4\psi))$.

3.4 A Fourth Order Convective Term: General Boundary Conditions

In the previous section we had a fourth-order approximation (3.25) for the convective term, based on the compact stencil and the Hermitian derivatives (ψ_x, ψ_y). In this section, we construct a fourth order approximation of the convective term for general boundary conditions, namely we do not impose periodic or no-leak conditions on the boundary as was needed for (3.25). However, the price to be paid is the use of higher order polynomials in order to compute approximate derivatives. Recall the definition of the convective term

$$u \cdot \partial_x \Delta\psi + v \cdot \partial_y \Delta\psi = -\partial_y\psi \Delta\partial_x\psi + \partial_x\psi \Delta\partial_y\psi. \tag{3.27}$$

Since the Hermitian gradient gives a fourth order approximation to $\partial_x\psi, \partial_y\psi$, we only need to have a fourth-order approximation to $\partial_x\Delta\psi$ and $\partial_y\Delta\psi$. Consider now

$$\partial_x\Delta\psi = \partial_x^3\psi + \partial_y^2\partial_x\psi. \tag{3.28}$$

We first construct a fourth order approximation to the pure third order derivative $\partial_x^3\psi$. Let us fix y to be y_j. We construct a fifth order polynomial in x, which interpolates ψ and $\partial_x\psi$ at $(x_{i-1}, y_j), (x_i, y_j), (x_{i+1}, y_j)$. The third order derivative of this polynomial at point (x_i, y_j) is

$$(\tilde{\psi}_{xxx})_{i,j} = \frac{3}{2h^2}\left(10\delta_x\psi_{i,j} - [(\partial_x\psi)_{i+1,j} + 8(\partial_x\psi)_{i,j} + (\partial_x\psi)_{i-1,j}]\right)$$

$$= \frac{3}{2h^2}\left(10\delta_x\psi - h^2\delta_x^2\partial_x\psi - 10\partial_x\psi\right)_{i,j}. \tag{3.29}$$

It can be easily checked that this defines a fourth order accurate approximation to $\partial_x^3\psi$ at (x_i, y_j), provided that $\partial_x\psi$ is the exact value of this partial derivative. In addition, the mixed third order derivative in (3.28) is approximated to fourth-order accuracy by $\tilde{\psi}_{yyx}$, where

$$\tilde{\psi}_{yyx} = \delta_y^2\partial_x\psi + \delta_x\delta_y^2\psi - \delta_x\delta_y\partial_y\psi. \tag{3.30}$$

This can be verified by a straightforward Taylor expansion. Therefore, combining 3.29)
and (3.30), we see that $\partial_x \Delta \psi$ is approximated to fourth order accuracy by

$$\widetilde{\partial_x \Delta_h} \psi = \frac{3}{2} \left(10 \frac{\delta_x \psi - \partial_x \psi}{h^2} - \delta_x^2 \partial_x \psi \right) + \delta_y^2 \partial_x \psi + \delta_x \delta_y^2 \psi - \delta_x \delta_y \partial_y \psi. \qquad (3.31)$$

Similarly, $\partial_y \Delta \psi$ is approximated by

$$\widetilde{\partial_y \Delta_h} \psi = \frac{3}{2} \left(10 \frac{\delta_y \psi - \partial_y \psi}{h^2} - \delta_y^2 \partial_y \psi \right) + \delta_x^2 \partial_y \psi + \delta_y \delta_x^2 \psi - \delta_y \delta_x \partial_x \psi. \qquad (3.32)$$

Thus, the convective term $-\psi_y \Delta_x \psi + \psi_y \Delta_y \psi$ is approximated by

$$\tilde{C}_h'(\psi) = -\psi_y \left(\frac{3}{2} \left(10 \frac{\delta_x \psi - \partial_x \psi}{h^2} - \delta_x^2 \partial_x \psi \right) + \delta_y^2 \partial_x \psi + \delta_x \delta_y^2 \psi - \delta_x \delta_y \partial_y \psi \right)$$
$$+ \psi_x \left(\frac{3}{2} \left(10 \frac{\delta_y \psi - \partial_y \psi}{h^2} - \delta_y^2 \partial_y \psi \right) + \delta_x^2 \partial_y \psi + \delta_y \delta_x^2 \psi - \delta_y \delta_x \partial_x \psi \right). \qquad (3.33)$$

Finally, (3.33) may be written as follows:

$$\tilde{C}_h'(\psi) = -\psi_y \left(\Delta_h \partial_x \psi + \frac{5}{2} \left(6 \frac{\delta_x \psi - \partial_x \psi}{h^2} - \delta_x^2 \partial_x \psi \right) + \delta_x \delta_y^2 \psi - \delta_x \delta_y \partial_y \psi \right)$$
$$+ \psi_x \left(\Delta_h \partial_y \psi + \frac{5}{2} \left(6 \frac{\delta_y \psi - \partial_y \psi}{h^2} - \delta_y^2 \partial_y \psi \right) + \delta_y \delta_x^2 \psi - \delta_y \delta_x \partial_x \psi \right)$$
$$= C(\psi) + O(h^4). \qquad (3.34)$$

Note that (3.34) is fourth-order accurate if ψ, $\partial_x \psi$ and $\partial_y \psi$ are the *exact values* of the
function ψ and its first order derivatives. However, if we approximate $\partial_x \psi$ and $\partial_y \psi$ by ψ_x
and ψ_y, which are defined by the Hermitian fourth-order relations

$$\delta_x \psi = \psi_x + \frac{h^2}{6} \delta_x^2 \psi_x, \qquad \delta_y \psi = \psi_y + \frac{h^2}{6} \delta_y^2 \psi_y, \qquad (3.35)$$

and substitute (3.35) in (3.34), then

$$\tilde{C}_h'(\psi) = -\psi_y \left(\Delta_h \psi_x + \delta_x \delta_y^2 \psi - \delta_x \delta_y \psi_y \right) + \psi_x \left(\Delta_h \psi_y + \delta_y \delta_x^2 \psi - \delta_y \delta_x \psi_x \right)$$
$$= C(\psi) + O(h^2). \qquad (3.36)$$

Observe that the latter is only second order accurate, whereas the loss of accuracy oc-
curs only due to the replacement of $(\partial_x \psi, \partial_y \psi)$ by (ψ_x, ψ_y) and $(\psi_x, \psi_y) = (\partial_x \psi +
O(h^4), \partial_y \psi + O(h^4))$. In order to retain fourth order accuracy in (3.34), when replacing
(∂_x, ∂_y) by approximate derivatives, we have to provide a sixth order approximation for
such derivatives. We denote the approximate derivatives by $\tilde{\psi}_x$ and $\tilde{\psi}_y$. Here we use a Padé
relation as given in [19]. It has the following form:

$$\frac{1}{3} (\tilde{\psi}_x)_{i+1,j} + (\tilde{\psi}_x)_{i,j} + \frac{1}{3} (\tilde{\psi}_x)_{i-1,j} = \frac{14}{9} \frac{\psi_{i+1,j} - \psi_{i-1,j}}{2h} + \frac{1}{9} \frac{\psi_{i+2,j} - \psi_{i-2,j}}{4h}. \qquad (3.37)$$

The local truncation error for $\tilde{\psi}_x$ in (3.37) is of sixth order, i.e.,

$$(\tilde{\psi}_x)_{i,j} = (\partial_x \psi)_{i,j} + h^6 \frac{1}{2100}(\partial_x^7 \psi)_{i,j} + O(h^8). \tag{3.38}$$

If we substitute (3.37) in (3.29) we obtain

$$(\tilde{\psi}_{xxx})_{i,j} = (\partial_x^3 \psi)_{i,j} + \frac{h^4}{120}(\partial_x^7 \psi)_{i,j} + O(h^6). \tag{3.39}$$

At near-boundary points we apply a one-sided approximation for $\partial_x \psi$ (see [19]). For $i = 1$ (a point next to the left boundary) we have

$$\frac{1}{10}(\tilde{\psi}_x)_{0,j} + \frac{6}{10}(\tilde{\psi}_x)_{1,j} + \frac{3}{10}(\tilde{\psi}_x)_{i-1,j} = \frac{-10\psi_{0,j} - 9\psi_{1,j} + 18\psi_{2,j} + \psi_{3,j}}{30h}. \tag{3.40}$$

For $i = N - 1$ we have

$$\frac{1}{10}(\tilde{\psi}_x)_{N,j} + \frac{6}{10}(\tilde{\psi}_x)_{N-1,j} + \frac{3}{10}(\tilde{\psi}_x)_{N-2,j} = \frac{10\psi_{N,j} + 9\psi_{N-1,j} - 18\psi_{N-2,j} - \psi_{N-3,j}}{30h}. \tag{3.41}$$

In a similar manner we approximate $\partial_y \psi$. To summarize, a fourth order approximation of the convective term for general boundary conditions is

$$\tilde{C}_h'(\psi) = -\psi_y \left(\Delta_h \tilde{\psi}_x + \frac{5}{2} \left(6\frac{\delta_x \psi - \tilde{\psi}_x}{h^2} - \delta_x^2 \tilde{\psi}_x \right) + \delta_x \delta_y^2 \psi - \delta_x \delta_y \tilde{\psi}_y \right)$$

$$+ \psi_x \left(\Delta_h \tilde{\psi}_y + \frac{5}{2} \left(6\frac{\delta_y \psi - \tilde{\psi}_y}{h^2} - \delta_y^2 \tilde{\psi}_y \right) + \delta_y \delta_x^2 \psi - \delta_y \delta_x \tilde{\psi}_x \right)$$

$$= C(\psi) + O(h^4), \tag{3.42}$$

where ψ_x, ψ_y are the Hermitian derivatives defined in (2.5) and $\tilde{\psi}_x, \tilde{\psi}_y$ are the approximate derivatives defined by the Padé relation for $2 \le i \le N - 2$, $1 \le j \le N - 1$, by

$$\begin{cases} \dfrac{1}{3}(\tilde{\psi}_x)_{i+1,j} + (\tilde{\psi}_x)_{i,j} + \dfrac{1}{3}(\tilde{\psi}_x)_{i-1,j} = \dfrac{14}{9}\dfrac{\psi_{i+1,j} - \psi_{i-1,j}}{2h} + \dfrac{1}{9}\dfrac{\psi_{i+2,j} - \psi_{i-2,j}}{4h}, \\[2mm] \dfrac{1}{10}(\tilde{\psi}_x)_{0,j} + \dfrac{6}{10}(\tilde{\psi}_x)_{1,j} + \dfrac{3}{10}(\tilde{\psi}_x)_{2,j} = \dfrac{-10\psi_{0,j} - 9\psi_{1,j} + 18\psi_{2,j} + \psi_{3,j}}{30h}, \\[2mm] \dfrac{1}{10}(\tilde{\psi}_x)_{N,j} + \dfrac{6}{10}(\tilde{\psi}_x)_{N-1,j} + \dfrac{3}{10}(\tilde{\psi}_x)_{N-2,j} = \dfrac{10\psi_{N,j} + 9\psi_{N-1,j} - 18\psi_{N-2,j} - \psi_{N-3,j}}{30h} \end{cases} \tag{3.43}$$

and $\tilde{\psi}_y$ is defined as a function of ψ for $1 \le i \le N - 1$, $2 \le j \le N - 2$ by

$$\begin{cases} \dfrac{1}{3}(\tilde{\psi}_y)_{i,j+1} + (\tilde{\psi}_y)_{i,j} + \dfrac{1}{3}(\tilde{\psi}_y)_{i,j-1} = \dfrac{14}{9}\dfrac{\psi_{i,j+1} - \psi_{i,j-1}}{2h} + \dfrac{1}{9}\dfrac{\psi_{i,j+2} - \psi_{i,j-2}}{4h}, \\[2mm] \dfrac{1}{10}(\tilde{\psi}_y)_{i,0} + \dfrac{6}{10}(\tilde{\psi}_y)_{i,1} + \dfrac{3}{10}(\tilde{\psi}_y)_{i,2} = \dfrac{-10\psi_{i,0} - 9\psi_{i,1} + 18\psi_{i,2} + \psi_{i,3}}{30h}, \\[2mm] \dfrac{1}{10}(\tilde{\psi}_y)_{i,N} + \dfrac{6}{10}(\tilde{\psi}_y)_{i,N-1} + \dfrac{3}{10}(\tilde{\psi}_y)_{i,N-2} = \dfrac{10\psi_{i,N} + 9\psi_{i,N-1} - 18\psi_{i,N-2} - \psi_{i,N-3}}{30h}. \end{cases} \tag{3.44}$$

Note that a compact scheme for irregular domains was developed in [10].

4 Time-Stepping Scheme

4.1 Introduction

Having approximated the spatial operators to fourth order accuracy in Sect. 3, we are left now with the semidiscrete dynamical system

$$\begin{cases} \partial_t \tilde{\Delta}_h \psi + C_h^{\text{app}}(\psi) - \nu \tilde{\Delta}_h^2 \psi = f(x_i, y_j, t), \\ \psi(x_i, y_j, t) = \psi_0(x_i, y_j). \end{cases} \tag{4.1}$$

Recall that:

- $\tilde{\Delta}_h \psi$ is the fourth order Laplacian (3.10)
- $\tilde{\Delta}_h^2 \psi$ is the fourth order approximation of the biharmonic (3.12)
- C_h^{app} is a fourth order approximation to the convective term $C(\psi)$ (see (3.22)). For example, we can take C_h^{app} as $\tilde{C}_h$ (see (3.25)) or C_h' (see (3.34)). That is

$$C_h^{\text{app}} = C(\psi) + O(h^4) = \nabla^\perp \psi \cdot \nabla \Delta \psi + O(h^4). \tag{4.2}$$

Using the notation

$$\begin{cases} U(t) = \tilde{\Delta}_h \psi(t), \\ D(t) = \nu \tilde{\Delta}_h^2(\psi(t)), \\ C(t) = C_h^{\text{app}}(\psi(t)), \\ F(t) = f(t), \end{cases} \tag{4.3}$$

we obtain the dynamical system

$$\frac{d}{dt} U(t) = -C(t) + D(t) + F(t). \tag{4.4}$$

We describe now two different one-level time-stepping schemes of IMplicit-EXplicit (IMEX) type (see [2, 3]). For IMEX schemes the convective term is treated explicitly, while the diffusive term is diagonally implicit.

4.2 Second Order Time-Stepping Scheme

The first IMEX scheme is the second order time-stepping scheme used in [7]. It is a one-level scheme with two intermediate steps, where each of them contains one resolution of a biharmonic problem. This scheme is explicit for the convective part and implicit for the diffusive part. We begin with the known quantity ψ^n and compute first $\psi^{n+1/2}$. We then use the intermediate quantity $\psi^{n+1/2}$ in a second step in order to obtain ψ^{n+1}. Letting U^1, D^1, C^1 be the quantities associated with ψ^n, similarly U^2, D^2, C^2 be the associated quantities associated with $\psi^{n+1/2}$ and U^3, D^3, C^3 be the associated quantities associated with ψ^{n+1}, the scheme may be written as follows.

$$\begin{cases} U^2 = U^1 + \dfrac{\Delta t}{2}\left(-C^1 + \dfrac{1}{2}D^1 + \dfrac{1}{2}D^2\right) + \dfrac{\Delta t}{2}\tilde{F}^{n+1/4}, \\ \\ U^3 = U^1 + \Delta t\left(-C^2 + \dfrac{1}{2}D^2 + \dfrac{1}{2}D^3\right) + \Delta t\,\tilde{F}^{n+1/2}. \end{cases} \tag{4.5}$$

Here $\psi^{n+1/2}$, ψ^{n+1} are involved (implicitly) in the expressions $U^2 - \frac{1}{2}\Delta t\, D^2$, $U^3 - \frac{1}{2}\Delta t\, D^3$, respectively. Note that the second step provides ψ^{n+1} as the solution of the problem

$$\left(\tilde{\Delta}_h - \frac{\Delta t}{2}\tilde{\Delta}_h^2\right)\psi^{n+1} = \tilde{\Delta}_h\psi^n + \Delta t\left(-C^2 + \frac{1}{2}D^2\right) + \Delta t\, F^{n+1/2}. \qquad (4.6)$$

This scheme is second order accurate in time and fourth order accurate in space. Namely, if ψ is the exact solution of (3.1), then it satisfies (4.6) up to an error $O((\Delta t)^3 + h^4)$. Finally, observe that we apply the fully-discrete scheme (4.5) at all interior points. On the boundaries, we impose the no-slip and no-leak boundary conditions. The latter completely determine ψ, ψ_x and ψ_y on the boundary.

4.3 Higher Order Time-Stepping Scheme

The second IMEX scheme to be described here is almost third order accurate. Note that the design of IMEX one-level stable schemes which is at least third order accurate is not an easy task (see [2]). This actually requires handling of the formal accuracy of the scheme in all Peclet regimes and the analysis of the restriction on the time step (i.e., a CFL condition) due to the convective term. Here we adopt a three-step Runge-Kutta scheme suggested in [49] in a slightly different context. Using the notation (see (4.3))

$$\begin{cases} U = \tilde{\Delta}_h\psi, \\ D = \nu\tilde{\Delta}_h^2(\psi), \\ C = C_h^{\text{app}}(\psi), \end{cases} \qquad (4.7)$$

and letting U^1, D^1, C^1 be the quantities associated with ψ^n (at the first time step), similarly U^2, D^2, C^2 be the associated quantities associated with ψ at the second time step, U^3, D^3, C^3 be the associated quantities associated with ψ at the third time step and U^4, D^4, C^4 be the quantities associated with ψ^{n+1}, the scheme reads

$$\begin{cases} U^2 = U^1 + \Delta t\left(\gamma_1(-C^1) + \alpha_1 D^1 + \beta_1 D^2\right) + \dfrac{8}{15}\Delta t\, F^{n+4/15}, \\[2mm] U^3 = U^2 + \Delta t\left(\gamma_2(-C^2) + \zeta_1(-C^1) + \alpha_2 D^2 + \beta_2 D^3\right) \\[2mm] \qquad\quad + \Delta t\left(\dfrac{2}{3}F^{n+1/3} - \dfrac{8}{15}F^{n+4/15}\right), \\[2mm] U^4 = U^3 + \Delta t\left(\gamma_3(-C^3) + \zeta_2(-C^2) + \alpha_3 D^3 + \beta_3 D^4\right) \\[2mm] \qquad\quad + \Delta t\left(\dfrac{1}{6}F^n + \dfrac{2}{3}F^{n+1/2} + \dfrac{1}{6}F^{n+1} - \dfrac{2}{3}F^{n+1/3}\right). \end{cases} \qquad (4.8)$$

The values of the parameters are as follows (see [49])

$$\begin{cases} \alpha_1 = \frac{29}{96}, & \alpha_2 = \frac{-3}{40}, & \alpha_3 = \frac{1}{6}, \\[1mm] \beta_1 = \frac{37}{160}, & \beta_2 = \frac{5}{24}, & \beta_3 = \frac{1}{6}, \\[1mm] \gamma_1 = \frac{8}{15}, & \gamma_2 = \frac{5}{12}, & \gamma_3 = \frac{3}{4}, \\[1mm] \zeta_1 = \frac{-17}{60}, & \zeta_2 = \frac{-5}{12}. \end{cases} \qquad (4.9)$$

The final value of ψ^{n+1} is obtained in the last step of the scheme, by solving

$$(\tilde{\Delta}_h - \Delta t \beta_3 \nu \tilde{\Delta}_h^2)\psi^{n+1} = U^3 + \Delta t \left(\gamma_3(-C^3) + \zeta_2(-C^2) + \alpha_3 D^3 \right)$$

$$+ \Delta t \left(\frac{1}{6} F^n + \frac{2}{3} F^{n+1/2} + \frac{1}{6} F^{n+1} - \frac{2}{3} F^{n+1/3} \right). \quad (4.10)$$

The values of the parameters in (4.9) were obtained by matching the Taylor expansion of the exact solution with the Taylor expansion of the solution derived by the time-stepping scheme. They satisfy the requirements for first and second order accuracy in time and all, except one, for third order accuracy in time. It is impossible to satisfy all these requirements in the setting of the scheme (4.8). Therefore, the formal accuracy of this time scheme is less than three (see [49]). Presumably, third order accuracy could be obtained by a four-step scheme. Note that in our numerical results third (or almost third) order accuracy in time was achieved (see Sect. 6 below).

5 Stability Analysis

5.1 Discrete Operators and Symbols

In this section, we consider the schemes (4.5) and (4.8) applied to the equation

$$\Delta \psi_t = C(\psi) + \nu \Delta^2 \psi, \quad (5.1)$$

where $C(\psi)$ is *a linear* convection term $C(\psi) = a \Delta \psi_x + b \Delta \psi_y$, with a, b being real constants. Note that for simplicity we take the convection term here to be the analog of $-C(t)$ in (4.4). Therefore, we consider the equation

$$\Delta \psi_t = a \Delta \psi_x + b \Delta \psi_y + \nu \Delta^2 \psi. \quad (5.2)$$

We perform the linear von-Neumann stability analysis, which consists of computing the amplification factor of the full discretized time-space scheme in the periodic setting over a uniform grid of mesh size h. We denote

$$\lambda = \sqrt{a^2 + b^2} \frac{\Delta t}{h} \quad \text{(the CFL number)}, \qquad \mu = \frac{\nu \Delta t}{h^2}. \quad (5.3)$$

The two phase angles in each of the directions x and y are $\theta = \alpha h \in [0, 2\pi)$ and $\varphi = \beta h \in [0, 2\pi)$. Every discrete operator (on ψ) is expressed (via the Fourier transformation) as a "symbol" multiplying the Fourier transform $\hat{\psi}$. Recall that the symbols of the Hermitian derivatives ψ_x, ψ_y (2.5) are

$$\widehat{\psi_x} = H_x \hat{\psi} = i \frac{3 \sin \theta}{h(2 + \cos \theta)} \hat{\psi}, \qquad \widehat{\psi_y} = H_y \hat{\psi} = i \frac{3 \sin \varphi}{h(2 + \cos \varphi)} \hat{\psi}, \quad (5.4)$$

respectively. Similarly, the symbols of the Padé derivatives $\tilde{\psi}_x$, $\tilde{\psi}_y$ (3.43) and (3.44) are

$$\widehat{\tilde{\psi}_x} = \tilde{H}_x \hat{\psi} = i \frac{\sin \theta (14 + \cos \theta)}{3h(3 + 2 \cos \theta)} \hat{\psi}, \qquad \widehat{\tilde{\psi}_y} = \tilde{H}_y \hat{\psi} = i \frac{\sin \varphi (14 + \cos \varphi)}{3h(3 + 2 \cos \varphi)} \hat{\psi}, \quad (5.5)$$

respectively. The symbols of $\delta_x \psi_x$ and $\delta_y \psi_y$ are

$$\widehat{\delta_x \psi_x} = K_x \hat{\psi} = -\frac{3\sin^2 \theta}{h^2(2+\cos\theta)} \hat{\psi}, \qquad \widehat{\delta_y \psi_y} = K_y \hat{\psi} = -\frac{3\sin^2 \varphi}{h^2(2+\cos\varphi)} \hat{\psi}, \qquad (5.6)$$

respectively. Similarly, the symbols of $\delta_x \tilde{\psi}_x, \delta_y \tilde{\psi}_y$ are

$$\widehat{\delta_x \tilde{\psi}_x} = \tilde{K}_x \hat{\psi} = -\frac{\sin^2 \theta (14+\cos\theta)}{3h^2(3+2\cos\theta)} \hat{\psi}, \qquad \widehat{\delta_y \tilde{\psi}_y} = \tilde{K}_y \hat{\psi} = -\frac{\sin^2 \varphi (14+\cos\varphi)}{3h^2(3+2\cos\varphi)} \hat{\psi}, \qquad (5.7)$$

respectively. We can now introduce the symbols of the discrete operators appearing in (4.5). The symbol of Δ_h is

$$M = -\frac{2}{h^2}((1-\cos\theta)+(1-\cos\varphi)). \qquad (5.8)$$

We compute next the symbol of the discrete fourth-order accurate Laplacian $\tilde{\Delta}_h$ (see (3.10)). Using (5.8) and (5.6), we find that the symbol of $-h^2 \tilde{\Delta}_h$, which we denote by $A_1(\theta, \varphi)$, is

$$A_1(\theta, \varphi) = \frac{(1-\cos\theta)(5+\cos\theta)}{2+\cos\theta} + \frac{(1-\cos\varphi)(5+\cos\varphi)}{2+\cos\varphi}. \qquad (5.9)$$

We turn next to the computation of the symbol of $\tilde{\Delta}_h^2 = \Delta_h^2 - \frac{h^2}{6}(\delta_x^2 \delta_y^4 + \delta_x^4 \delta_y^2)$, which is the discrete fourth-order accurate biharmonic operator (3.12). We note that the symbols of δ_x^4 and δ_y^4 (see (2.8) and (2.9)) are respectively

$$J_x = \frac{12}{h^4} \frac{(1-\cos\theta)^2}{2+\cos\theta}, \qquad J_y = \frac{12}{h^4} \frac{(1-\cos\varphi)^2}{2+\cos\varphi}, \qquad (5.10)$$

(see (5.6) for $\widehat{\delta_x \psi_x}$ and $\widehat{\delta_y \psi_y}$). Therefore, the symbol of $h^2 \nu \tilde{\Delta}_h^2$, which is denoted by $B_1(\theta, \varphi)$, is

$$\begin{aligned} B_1(\theta, \varphi) &= h^2 \nu \left(J_x + J_y + \frac{4}{h^4}(1-\cos\theta)\left(1-\cos\varphi + \frac{h^4}{12}J_y\right) \right. \\ &\quad \left. + \frac{4}{h^4}(1-\cos\varphi)\left(1-\cos\theta + \frac{h^4}{12}J_x\right) \right) \\ &= 12\nu h^{-2}\left(\frac{(1-\cos\theta)^2}{2+\cos\theta} + \frac{(1-\cos\varphi)^2}{2+\cos\varphi} \right. \\ &\quad \left. + (1-\cos\theta)(1-\cos\varphi)\left(\frac{1}{2+\cos\varphi} + \frac{1}{2+\cos\theta} \right) \right). \qquad (5.11) \end{aligned}$$

The convective term approximations in the case of (5.2) are given by the following analogues of (3.25) and (3.42):

$$\tilde{C}_h(\psi) = a\Delta_h \psi_x + b\Delta_h \psi_y - \frac{h^2}{12}\left(a\delta_x(\delta_x^4 + \delta_y^4) + b\delta_y(\delta_x^4 + \delta_y^4)\right)\psi, \qquad (5.12)$$

where (ψ_x, ψ_y) is the Hermitian approximation (2.6), (2.7) to $\nabla\psi$ at grid points and

$$\tilde{C}'_h(\psi) = a\left(\Delta_h\tilde{\psi}_x + \frac{5}{2}\left(6\frac{\delta_x\psi - \tilde{\psi}_x}{h^2} - \delta_x^2\tilde{\psi}_x\right) + \delta_x\delta_y^2\psi - \delta_x\delta_y\tilde{\psi}_y\right)$$

$$+ b\left(\Delta_h\tilde{\psi}_y + \frac{5}{2}\left(6\frac{\delta_y\psi - \tilde{\psi}_y}{h^2} - \delta_y^2\tilde{\psi}_y\right) + \delta_y\delta_x^2\psi - \delta_y\delta_x\tilde{\psi}_x\right), \quad (5.13)$$

where $\tilde{\psi}_x$, $\tilde{\psi}_y$ are the approximate Padé derivatives defined in (3.43) and (3.44).

(I) *The symbol of* $\tilde{C}_h$ (see (5.12)): Note that $\tilde{C}_h(\psi)$ is fourth-order accurate in the case of periodic (or no-leak) boundary conditions. The symbols of the operators $\psi \to \Delta_h\psi_x$ and $\psi \to \Delta_h\psi_y$ are

$$M_x = MH_x = -i\frac{6\sin\theta}{h^3(2+\cos\theta)}((1-\cos\theta) + (1-\cos\varphi)),$$

$$M_y = MH_y = -i\frac{6\sin\varphi}{h^3(2+\cos\varphi)}((1-\cos\theta) + (1-\cos\varphi)) \quad (5.14)$$

and the symbols of $\psi \to \delta_x(\delta_x^4\psi + \delta_y^4\psi)$ and $\psi \to \delta_y(\delta_x^4\psi + \delta_y^4\psi)$ are

$$N_x = i\frac{\sin\theta}{h}(J_x + J_y) = i\frac{12\sin\theta}{h^5}\left(\frac{(1-\cos\theta)^2}{2+\cos\theta} + \frac{(1-\cos\varphi)^2}{2+\cos\varphi}\right),$$

$$N_y = i\frac{\sin\varphi}{h}(J_x + J_y) = i\frac{12\sin\varphi}{h^5}\left(\frac{(1-\cos\varphi)^2}{2+\cos\varphi} + \frac{(1-\cos\varphi)^2}{2+\cos\varphi}\right). \quad (5.15)$$

Denote by $C_1(\theta,\varphi)$ the symbol of $ih^2\tilde{C}_h$. From (5.12), (5.14) and (5.15) we obtain

$$C_1(\theta,\varphi) = h^{-1}\left(a\sin\theta\left((1-\cos\theta)\frac{7-\cos\theta}{2+\cos\theta} + (1-\cos\varphi)\left(\frac{6}{2+\cos\theta} + \frac{1-\cos\varphi}{2+\cos\varphi}\right)\right)\right.$$

$$\left. + b\sin\varphi\left((1-\cos\varphi)\frac{7-\cos\varphi}{2+\cos\varphi} + (1-\cos\theta)\left(\frac{6}{2+\cos\varphi} + \frac{1-\cos\theta}{2+\cos\theta}\right)\right)\right). \quad (5.16)$$

Note also that

$$C_1^2(\theta,\varphi) \leq h^{-2}(a^2 + b^2)\tilde{D}(\theta,\varphi), \quad (5.17)$$

where

$$\tilde{D}(\theta,\varphi) = \left\{|\sin\theta|\left((1-\cos\theta)\frac{7-\cos\theta}{2+\cos\theta} + (1-\cos\varphi)\left(\frac{6}{2+\cos\theta} + \frac{1-\cos\varphi}{2+\cos\varphi}\right)\right)\right\}^2$$

$$+ \left\{|\sin\varphi|\left((1-\cos\varphi)\frac{7-\cos\varphi}{2+\cos\varphi} + (1-\cos\theta)\left(\frac{6}{2+\cos\varphi} + \frac{1-\cos\theta}{2+\cos\theta}\right)\right)\right\}^2. \quad (5.18)$$

(II) *The symbol of* $\bar{C}'_h$ (see (5.13), *which is the analogue of* (3.42)): Recall that $\tilde{C}'_h(\psi)$ is fourth order accurate in the case of general boundary conditions. The symbols of $\psi \to \Delta_h\tilde{\psi}_x$

and $\psi \to \Delta_h \tilde{\psi}_y$ are

$$
\begin{aligned}
L_x = M\tilde{H}_x &= -i\frac{2\sin\theta(14+\cos\theta)}{3h^3(3+2\cos\theta)}((1-\cos\theta+(1-\cos\varphi)), \\
L_y = M\tilde{H}_y &= -i\frac{2\sin\varphi(14+\cos\varphi)}{3h^3(3+2\cos\varphi)}((1-\cos\theta+(1-\cos\varphi))
\end{aligned}
\tag{5.19}
$$

and the symbols of $\psi \to \frac{5}{2}(6\frac{\delta_x\psi-\tilde{\psi}_x}{h^2} - \delta_x^2\tilde{\psi}_x)$, $\psi \to \frac{5}{2}(6\frac{\delta_y\psi-\tilde{\psi}_y}{h^2} - \delta_y^2\tilde{\psi}_y)$ are

$$
I_x = -i\frac{5\sin\theta(1-\cos\theta)^2}{3h^3(3+2\cos\theta)}, \qquad I_y = -i\frac{5\sin\varphi(1-\cos\varphi)^2}{3h^3(3+2\cos\varphi)}.
\tag{5.20}
$$

In addition, the symbols of $\psi \to \delta_x\delta_y^2\psi$, $\psi \to \delta_y\delta_x^2\psi$ are

$$
Q_x = -i\frac{2\sin\theta(1-\cos\varphi)}{h^3}, \qquad Q_y = -i\frac{2\sin\varphi(1-\cos\theta)}{h^3}
\tag{5.21}
$$

and the symbols of $\delta_x\delta_y\tilde{\psi}_y$, $\delta_y\delta_x\tilde{\psi}_x$ are

$$
\begin{aligned}
R_x &= i\frac{\sin\theta}{h}\tilde{K}_y = -i\frac{\sin\theta\sin^2\varphi(14+\cos\varphi)}{3h^3(3+2\cos\varphi)}, \\
R_y &= i\frac{\sin\varphi}{h}\tilde{K}_x = -i\frac{\sin\varphi\sin^2\theta(14+\cos\theta)}{3h^3(3+2\cos\theta)}.
\end{aligned}
\tag{5.22}
$$

Denote by $C_1'(\theta,\varphi)$ the symbol of $ih^2\tilde{C}_h'(\psi)$. From (5.13), (5.19), (5.20), (5.21) and (5.22) we obtain

$$
C_1'(\theta,\varphi) = h^{-1}\left(aG(\theta,\varphi) + bG(\varphi,\theta)\right),
\tag{5.23}
$$

where

$$
\begin{aligned}
G(\theta,\varphi) = \sin\theta\bigg(&(1-\cos\theta)\frac{11-\cos\theta}{3+2\cos\theta} \\
&+ (1-\cos\varphi)\left(\frac{2(23+7\cos\theta)}{3(3+2\cos\theta)} - \frac{(1+\cos\varphi)(14+\cos\varphi)}{3(3+2\cos\varphi)}\right)\bigg).
\end{aligned}
\tag{5.24}
$$

5.2 Stability of the Second Order Time-Stepping Scheme

In this section we analyze the stability of the second order time-stepping scheme with the two different approximations for the convective term $\tilde{C}_h$, or $\tilde{C}_h'$.

The second order time-stepping scheme (4.5) reads, with, for example $\tilde{C}_h$:

- Step 1: Computation of $\psi^{n+1/2}$

$$
\left(\tilde{\Delta}_h - \frac{1}{4}\Delta t\nu\tilde{\Delta}_h^2\right)\psi^{n+1/2} = \left(\tilde{\Delta}_h\psi^n + \frac{1}{4}\Delta t\nu\tilde{\Delta}_h^2\right)\psi^n + \frac{1}{2}\Delta t\tilde{C}_h(\psi^n).
\tag{5.25}
$$

- Step 2: Computation of ψ^{n+1}

$$
\left(\tilde{\Delta}_h - \frac{1}{2}\Delta t\nu\tilde{\Delta}_h^2\right)\psi^{n+1} = \left(\tilde{\Delta}_h\psi^n + \frac{1}{2}\Delta t\nu\tilde{\Delta}_h^2\right)\psi^n + \Delta t\tilde{C}_h(\psi^{n+1/2}).
\tag{5.26}
$$

The second order time-stepping scheme has already been used in our work [7] but with second order spatial operators Δ_h, Δ_h^2, C_h instead of the fourth order spatial operators $\tilde{\Delta}_h$, $\tilde{\Delta}_h^2$, $\tilde{C}_h$ (or $\tilde{C}_h'$). Here we improve the accuracy of the spatial operators and also the stability criterion as follows.

5.2.1 Stability Condition on the Time-Step

The stability analysis carried out in this subsection reveals a surprising fact:

A sufficient condition for the stability of the scheme is

$$(a^2 + b^2)\Delta t \leq C\nu,$$

where $C > 0$ is a numerical constant (which is explicitly calculated below).

In particular, this condition is independent of h and implies the unconditional stability of the scheme when $a = b = 0$.

The following proposition gives a sufficient stability condition on the time-step for the scheme (5.25) for each of the two convective terms $\tilde{C}_h$ and $\tilde{C}_h'$.

Proposition 5.1

(i) (Convective term for no-leak boundary condition (5.12)) *The predictor-corrector scheme (5.25, 5.26) is stable in the von-Neumann sense under the sufficient condition*

$$24(a^2 + b^2)\Delta t \leq \nu. \tag{5.27}$$

(ii) (Convective term for general boundary condition (5.13)) *The predictor-corrector scheme (5.25, 5.26) is stable in the von-Neumann sense under the sufficient condition*

$$54(a^2 + b^2)\Delta t \leq \nu. \tag{5.28}$$

Proof We perform the proof of (i) only, as the proof of (ii) goes along the same lines. Let $g_1(\theta, \varphi)$, $g_2(\theta, \varphi)$ be the amplification factors related to (5.25, 5.26), respectively. We have

$$
\begin{cases}
g_1(\theta, \varphi) = \dfrac{A_1(\theta, \varphi) - \frac{\Delta t}{4}B_1(\theta, \varphi) + i\frac{\Delta t}{2}C_1(\theta, \varphi)}{A_1(\theta, \varphi) + \frac{\Delta t}{4}B_1(\theta, \varphi)}, \\[4mm]
g_2(\theta, \varphi) = \dfrac{A_1(\theta, \varphi) - \frac{\Delta t}{2}B_1(\theta, \varphi) + i\,\Delta t\, C_1(\theta, \varphi)g_1(\theta, \varphi)}{A_1(\theta, \varphi) + \frac{\Delta t}{2}B_1(\theta, \varphi)}.
\end{cases}
\tag{5.29}
$$

Note that g_2 is the amplification factor for the full time-step.

The (strong) von-Neumann stability condition is (see [51])

$$\sup_{\theta,\varphi\in[0,2\pi)} |g_2(\theta, \varphi)| \leq 1. \tag{5.30}$$

We restrict ourselves to the case where

$$\sup_{\theta,\varphi\in[0,2\pi)} |g_1(\theta, \varphi)| \leq 1. \tag{5.31}$$

This is equivalent to

$$\Delta t\, C_1^2 \leq 4A_1 B_1. \tag{5.32}$$

In order to study the meaning of this condition in terms of Δt, we define new variables

$$x = \sin\frac{\theta}{2}, \qquad y = \sin\frac{\varphi}{2}. \tag{5.33}$$

Then

$$\begin{aligned} A_1 &\geq 4(x^2 + y^2), \\ B_1 &\geq 16vh^{-2}(x^4 + y^4 + 2x^2 y^2) = 16vh^{-2}(x^2 + y^2)^2, \end{aligned} \tag{5.34}$$

$$|C_1| \leq 32h^{-1}(|ax| + |by|)(x^2 + y^2). \tag{5.35}$$

The condition (5.32) is therefore implied by

$$32^2 \Delta t\, h^{-2}(|ax| + |by|)^2 (x^2 + y^2)^2 \leq 16^2 vh^{-2}(x^2 + y^2)^3, \tag{5.36}$$

or

$$4\Delta t\, (|ax| + |by|)^2 \leq v(x^2 + y^2). \tag{5.37}$$

This condition is implied in turn by

$$4(a^2 + b^2)\Delta t \leq v. \tag{5.38}$$

From now on we assume that (5.31) holds. Then, (5.30) is satisfied if

$$-2\Delta t C_1(\theta, \varphi)\, \mathrm{Im}(g_1(\theta, \varphi))\left[A_1(\theta, \varphi) - \frac{\Delta t}{2}B_1(\theta, \varphi)\right] + (\Delta t)^2 C_1^2(\theta, \varphi)|g_1(\theta, \varphi)|^2$$

$$\leq 2\Delta t A_1(\theta, \varphi)B_1(\theta, \varphi), \quad (\theta, \varphi) \in [0, 2\pi]^2. \tag{5.39}$$

Inserting the value of $\mathrm{Im}(g_1(\theta, \varphi))$ from (5.29) we conclude that a sufficient condition for (5.30) is

$$(\Delta t)^2 C_1^2 \left(1 - \frac{A_1 - \frac{\Delta t}{2}B_1}{A_1 + \frac{\Delta t}{4}B_1}\right) \leq 2\Delta t A_1 B_1, \tag{5.40}$$

which is satisfied if and only if

$$(\Delta t)^2 C_1^2 \leq \frac{8}{3}\left(A_1^2 + \frac{\Delta t}{4}A_1 B_1\right). \tag{5.41}$$

Ignoring the term A_1^2 in the right-hand side we finally obtain the sufficient condition

$$(\Delta t)^2 C_1^2 \leq \frac{2\Delta t}{3}A_1 B_1. \tag{5.42}$$

This leads (see (5.38)) to

$$24(a^2 + b^2)\Delta t \leq v.$$

This completes the proof of the proposition. □

Remark 5.2 (Concerning more general stability analysis) (a) Observe that in the nonconvective case, $a = b = 0$, the scheme is unconditionally stable. In the presence of the convective term the time step should be limited by the viscosity coefficient.

(b) Note that the stability result in Proposition 5.1 obtained for a convective term $C(\psi)$ as in (5.2), i.e., constant coefficients. If a, b are replaced by *known functions u, v*, we obtain the linearized form of the Navier-Stokes system. The stability analysis in this case cannot be carried out by the von-Neumann "amplification factor" method, and one must resort to some energy L^2 estimates. In fact, using the coercivity of the biharmonic term, this was done in [8], even for the *fully nonlinear* case, when the discretized form of the convective term was second-order accurate. In our treatment here we insist on *fourth-order accuracy* of the convective term (see Sects. 3.3, 3.4). It is not clear yet how the coercivity of the biharmonic operator can be used in order to majorize the (linearized) convective term of order four in (3.25) or (3.33). Furthermore using the general pattern of the von-Neumann analysis, we have used periodic boundary conditions. Using the more realistic no-leak condition complicates considerably the analysis, even though we expect the main conclusion in Proposition 5.1 (i.e., dependence of Δt on ν) to remain valid.

(c) Finally recall that, using a general framework, one can derive convergence rates from the accuracy estimates. Indeed, let us consider an exact equation

$$\frac{\partial \psi}{\partial t} = L\psi, \tag{5.43}$$

and its approximate version

$$\frac{\partial \psi}{\partial t} = L_h \psi. \tag{5.44}$$

The stability implies that $\exp(L_h t)$ is uniformly bounded (in $h > 0$), for $0 \leq t \leq T$.

Thus, if

$$\|L\phi - L_h\phi\| \leq C(\phi)h^\beta, \tag{5.45}$$

then also

$$\|\exp(Lt)\phi - \exp(L_h t)\phi\| \leq C(\phi, T)h^\beta, \quad 0 \leq t \leq T. \tag{5.46}$$

It follows that for (5.2), with *periodic boundary conditions,* the semi-discrete (in time) evolution converges at a fourth-order (with respect to h) rate. If a fully discrete version is employed, then the rate of convergence will also depend on the accuracy (with respect to Δt) of the time discretization. We refer to [27] for the fourth-order convergence analysis in the streamfunction-vorticity formulation and to [8] for the pure streamfunction formulation. Observe that both these papers address the convergence of the fully nonlinear system.

5.2.2 Dimensionless Stability Analysis

In this subsection, we analyze the stability condition for the scheme (5.25, 5.26) in terms of the dimensionless numbers λ and μ, see (5.3).

First, observe that if we keep the term A_1^2 in (5.41) then we can improve the stability condition in the following way. Note that (5.16) implies

$$|C_1| \leq 16h^{-1}(|a \sin \theta| + |b \sin \varphi|)(x^2 + y^2). \tag{5.47}$$

By (5.34) and (5.47), we obtain that (5.41) is implied by

$$16^2 \left(\frac{\Delta t}{h} \right)^2 (|a \sin \theta| + |b \sin \varphi|)^2 \leq \frac{8}{3} (16 + 16\mu(x^2 + y^2)). \tag{5.48}$$

Thus, a sufficient condition for (5.41) is

$$\lambda^2 \leq \frac{1}{12} + \frac{1}{24}\mu. \tag{5.49}$$

Taking into account (5.38), we find that a sufficient condition for overall stability is

$$\lambda^2 \leq \min\left(\frac{1}{4}\mu, \frac{1}{12} + \frac{1}{24}\mu \right) := CFL_1^2(\mu). \tag{5.50}$$

Similarly, for the convective term $\tilde{C}'_h$, we have

$$\lambda^2 \leq \min\left(\frac{1}{9}\mu, \frac{1}{27} + \frac{1}{54}\mu \right). \tag{5.51}$$

Looking at the right-hand side of (5.50), we distinguish between two different cases for which the minimum is achieved:

- $\mu \leq \frac{2}{5}$. In this case, we are computationally in the diffusive regime. The stability condition (5.50) reads

$$\lambda \leq \frac{1}{2}\sqrt{\mu}, \tag{5.52}$$

  or equivalently

$$\Delta t \leq \frac{\nu}{4(a^2 + b^2)}, \tag{5.53}$$

  which is (5.38). In particular, this means that if $\nu \to 0^+$, then the time step tends to zero independently of the mesh size h.
- $\mu > \frac{2}{5}$. In this case, the stability condition becomes

$$\lambda \leq \sqrt{\frac{1}{12} + \frac{1}{24}\mu}. \tag{5.54}$$

A sufficient condition for stability, which is uniform for all $\mu \geq \frac{2}{5}$, is $\lambda \leq \frac{1}{\sqrt{10}}$. Equivalently

$$\Delta t \leq \frac{h}{\sqrt{10(a^2 + b^2)}}. \tag{5.55}$$

In addition, we would like to give a practical interpretation of the stability condition (5.50). For this purpose, we restrict ourselves to a sufficient condition, which is more restrictive then (5.50), namely:

$$\lambda^2 \leq \min\left(\frac{1}{4}\mu, \frac{1}{12} \right). \tag{5.56}$$

Fig. 1 Curves
$\text{Log}(\mu) \mapsto \text{Log}(CFL_1(\mu))$ with
'−' (theoretical) and
$\text{Log}(\mu) \mapsto \text{Log}(CFL_2(\mu))$ with
'o' (numerical)
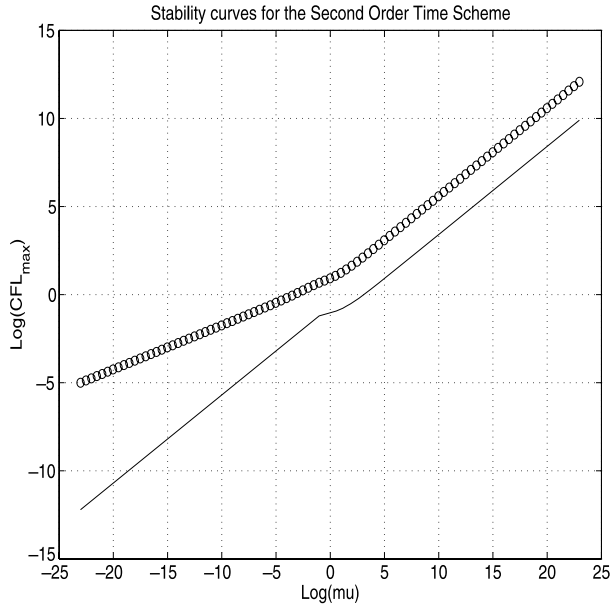
This means that a sufficient condition for stability is

$$\Delta t \leq \min\left(\frac{1}{4(a^2 + b^2)} \nu, \frac{1}{\sqrt{12(a^2 + b^2)}} h \right). \tag{5.57}$$

Therefore, for small ν the time step Δt is restricted by a factor of ν and for larger ν the time step is restricted by a factor of h.

In Fig. 1 we display the stability curve

$$\mu > 0 \mapsto CFL_1(\mu), \tag{5.58}$$

where $CFL_1(\mu)$ is defined in (5.50). In order to provide a more accurate view of the stability condition (5.50) for the scheme (5.25, 5.26), we also computed numerically the curve

$$\mu > 0 \mapsto CFL_2(\mu), \tag{5.59}$$

where $CFL_2(\mu)$ is the maximum value defined by the stability condition (5.30) alone, without the intermediate assumption (5.31). Inserting in the expression for g_2 the expression for g_1, we obtain that (5.30) is equivalent to

$$\bar{C}_1^4 + \bar{B}_1\left(\frac{3}{4}\bar{B}_1 - A_1 \right)\bar{C}_1^2 - 2A_1\bar{B}_1\left(2A_1 + \frac{1}{2}\bar{B}_1 \right)^2 \leq 0 \quad \forall (\theta, \varphi) \in [0, 2\pi)^2, \tag{5.60}$$

where

$$\bar{B}_1 = \Delta t\, B_1, \qquad \bar{C}_1 = \Delta t\, C_1 \tag{5.61}$$

are the dimensionless symbols of the biharmonic and convective terms. The discriminant of the second order polynomial, which appears in (5.60), considered as a function of $\bar{C}_1^2$ is

$$\Delta(\theta, \varphi, \mu) = \bar{B}_1^2 \left(\frac{3\bar{B}_1}{4} - A_1 \right)^2 + 8 A_1 \bar{B}_1 \left(2 A_1 + \frac{1}{2} \bar{B}_1 \right)^2 \geq 0. \qquad (5.62)$$

The two roots of the second order polynomial in (5.60), considered as a function of $\bar{C}_1^2$, have opposite sign. Therefore, a sufficient condition for (5.60) to hold is that

$$\bar{C}_1^2 \leq \frac{1}{2} \left(\bar{B}_1 \left(A_1 - \frac{3}{4} \bar{B}_1 \right) + \sqrt{\Delta} \right) := N(\theta, \varphi, \mu), \qquad (5.63)$$

Combining (5.63) with (5.17), we obtain that a sufficient stability condition is

$$\lambda^2 \leq \min_{0 < \theta, \varphi < 2\pi} \frac{N(\theta, \varphi, \mu)}{\tilde{D}(\theta, \varphi)} := CFL_2^2(\mu), \qquad (5.64)$$

where $\tilde{D}(\theta, \varphi)$ is defined in (5.18). Sampling μ in some interval $[0, \mu_{\max}]$, we compute numerically, as before, the minimum appearing in the right-hand side of (5.64). In Fig. 1 we report the two Log Log plots of the functions $\mu > 0 \mapsto CFL_1(\mu), CFL_2(\mu)$. Observe that as expected, the curves satisfy

$$CFL_1(\mu) < CFL_2(\mu) \qquad (5.65)$$

and that they have a similar shape.

5.3 Stability of the High Order Time-Stepping Scheme

We consider here the scheme (4.8) for the linear equation (5.2). The three steps to compute ψ^{n+1} as a function of $\psi^n = \psi^{(1)}$ are:

- *Step* 1: Computation of $\psi^{(2)}$

$$(\tilde{\Delta}_h - \beta_1 \Delta t \nu \tilde{\Delta}_h^2) \psi^{(2)} = (\tilde{\Delta}_h \psi^{(1)} + \alpha_1 \Delta t \nu \tilde{\Delta}_h^2) \psi^{(1)} + \gamma_1 \Delta t \tilde{C}_h (\psi^{(1)} \qquad (5.66)$$

- *Step* 2: Computation of $\psi^{(3)}$

$$(\tilde{\Delta}_h - \beta_2 \Delta t \nu \tilde{\Delta}_h^2) \psi^{(3)} = (\tilde{\Delta}_h \psi^{(2)} + \alpha_2 \Delta t \nu \tilde{\Delta}_h^2) \psi^{(2)} + \gamma_2 \Delta t \tilde{C}_h (\psi^{(2)}) + \zeta_1 \Delta t \tilde{C}_h (\psi^{(1)}) \qquad (5.67)$$

- *Step* 3: Computation of $\psi^{(4)}$

$$(\tilde{\Delta}_h - \beta_3 \Delta t \nu \tilde{\Delta}_h^2) \psi^{(4)} = (\tilde{\Delta}_h \psi^{(3)} + \alpha_3 \Delta t \nu \tilde{\Delta}_h^2) \psi^{(3)} + \gamma_3 \Delta t \tilde{C}_h (\psi^{(3)}) + \zeta_2 \Delta t \tilde{C}_h (\psi^{(2)}). \qquad (5.68)$$

The three amplification factors, corresponding respectively to the three steps are $(\theta, \varphi) \mapsto g_1(\theta, \varphi), g_2(\theta, \varphi), g_3(\theta, \varphi)$

$$\begin{cases} g_1 = \dfrac{A_1 - \alpha_1 \bar{B}_1 + i \gamma_1 \bar{C}_1}{A_1 + \beta_1 \bar{B}_1}, \\[3mm] g_2 = \dfrac{(A_1 - \alpha_2 \bar{B}_1) g_1 + i(\gamma_2 g_1 + \zeta_1) \bar{C}_1}{A_1 + \beta_2 \bar{B}_1}, \\[3mm] g_3 = \dfrac{(A_1 - \alpha_3 \bar{B}_1) g_2 + i(\gamma_3 g_2 + \zeta_2 g_1) \bar{C}_1}{A_1 + \beta_3 \bar{B}_1}, \end{cases} \qquad (5.69)$$

where $\bar{B}_1$ and $\bar{C}_1$ are as in (5.61). The von-Neumann stability condition linking μ and λ is

$$\max_{\theta,\varphi\in[0,2\pi)} |g_3(\theta,\varphi)| \leq 1. \tag{5.70}$$

We note that $|g_3| \leq 1$ is equivalent to

$$\begin{aligned}
&\left[(A_1 - \alpha_3\bar{B}_1)\operatorname{Re}(g_2) - C_1(\gamma_3\operatorname{Im}(g_2) + \zeta_2\operatorname{Im}(g_1))\right]^2 \\
&\quad + \left[(A_1 - \alpha_3\bar{B}_1)\operatorname{Im}(g_2) + C_1(\gamma_3\operatorname{Re}(g_2) + \zeta_2\operatorname{Re}(g_1))\right]^2 \\
&\quad \leq (A_1 + \beta_3\bar{B}_1)^2.
\end{aligned} \tag{5.71}$$

We compute now the real and the imaginary parts of g_1 and g_2:

$$\operatorname{Re}(g_1) = \frac{A_1 - \alpha_1\bar{B}_1}{A_1 + \beta_1\bar{B}_1}, \qquad \operatorname{Im}(g_1) = \frac{\gamma_1\bar{C}_1}{A_1 + \beta_1\bar{B}_1}, \tag{5.72}$$

$$\operatorname{Re}(g_2) = \frac{(A_1 - \alpha_2\bar{B}_1)(A_1 - \alpha_1\bar{B}_1) - \gamma_1\gamma_2\bar{C}_1^2}{(A_1 + \beta_1\bar{B}_1)(A_1 + \beta_2\bar{B}_1)}, \tag{5.73}$$

$$\operatorname{Im}(g_2) = C_1\frac{(\zeta_1 + \gamma_1 + \gamma_2)A_1 - (\alpha_2\gamma_1 + \alpha_1\gamma_2 - \beta_1\zeta_1)\bar{B}_1}{(A_1 + \beta_1\bar{B}_1)(A_1 + \beta_2\bar{B}_1)}. \tag{5.74}$$

Inserting the real and the imaginary parts of g_1 and g_2 in (5.71), we find that a sufficient condition for stability is

$$\begin{aligned}
&\left[(A_1 - \alpha_3\bar{B}_1)(A_1 - \alpha_2\bar{B}_1)(A_1 - \alpha_1\bar{B}_1) - \gamma_1\gamma_2(A_1 - \alpha_3\bar{B}_1)\bar{C}_1^2 \right. \\
&\quad \left. - \gamma_3\bar{C}_1^2\big((\zeta_1 + \gamma_1 + \gamma_2)A_1 - (\alpha_2\gamma_1 + \alpha_1\gamma_2 - \beta_1\zeta_1)\bar{B}_1\big) - \gamma_1\zeta_2\bar{C}_1^2(A_1 + \beta_2\bar{B}_1)\right]^2 \\
&\quad + \bar{C}_1^2\big[(A_1 - \alpha_3\bar{B}_1)((\zeta_1 + \gamma_1 + \gamma_2)A_1 - (\alpha_2\gamma_1 + \alpha_1\gamma_2 - \beta_1\zeta_1)\bar{B}_1) \\
&\quad + \gamma_3(A_1 - \alpha_1\bar{B}_1)(A_1 - \alpha_2\bar{B}_1) - \gamma_1\gamma_2\gamma_3\bar{C}_1^2 + \zeta_2(A_1 - \alpha_1\bar{B}_1)(A_1 + \beta_2\bar{B}_1)\big]^2 \\
&\quad \leq (A_1 + \beta_1\bar{B}_1)^2(A_1 + \beta_2\bar{B}_1)^2(A_1 + \beta_3\bar{B}_1)^2.
\end{aligned} \tag{5.75}$$

Expanding the left-hand side of the last inequality as a polynomial in $\bar{C}_1^2$, we find that $|g_3| \leq 1$ is equivalent to

$$(A - \bar{C}_1^2 B)^2 + \bar{C}_1^2(D - \bar{C}_1^2 E)^2 - F \leq 0, \tag{5.76}$$

where A, B, D, E, F are defined as functions of θ, φ and μ by

$$\begin{cases}
A = (A_1 - \alpha_1\bar{B}_1)(A_1 - \alpha_2\bar{B}_1)(A_1 - \alpha_3\bar{B}_1), \\
B = (\gamma_1\gamma_2 + \gamma_2\gamma_3 + \gamma_3\gamma_1 + \gamma_1\zeta_2 + \gamma_3\zeta_1)A_1 \\
\quad + (\gamma_1\zeta_2\beta_2 + \gamma_3\zeta_1\beta_1 - \gamma_1\gamma_2\alpha_3 - \gamma_3\gamma_1\alpha_2 - \gamma_2\gamma_3\alpha_1)\bar{B}_1, \\
D = (A_1 - \alpha_3\bar{B}_1)\big((\gamma_1 + \gamma_2 + \zeta_1)A_1 + (\beta_1\zeta_1 - \alpha_2\gamma_1 - \alpha_1\gamma_2)\bar{B}_1\big) \\
\quad + (A_1 - \alpha_1\bar{B}_1)\big((\gamma_3 + \zeta_2)A_1 + (\zeta_2\beta_2 - \gamma_3\alpha_2)\bar{B}_1\big), \\
E = \gamma_1\gamma_2\gamma_3, \\
F = (A_1 + \beta_1\bar{B}_1)^2(A_1 + \beta_2\bar{B}_1)^2(A_1 + \beta_3\bar{B}_1)^2.
\end{cases} \tag{5.77}$$

Fig. 2 Curve
$\text{Log}(\mu) \mapsto \text{Log}(CFL_3(\mu))$
with 'o'
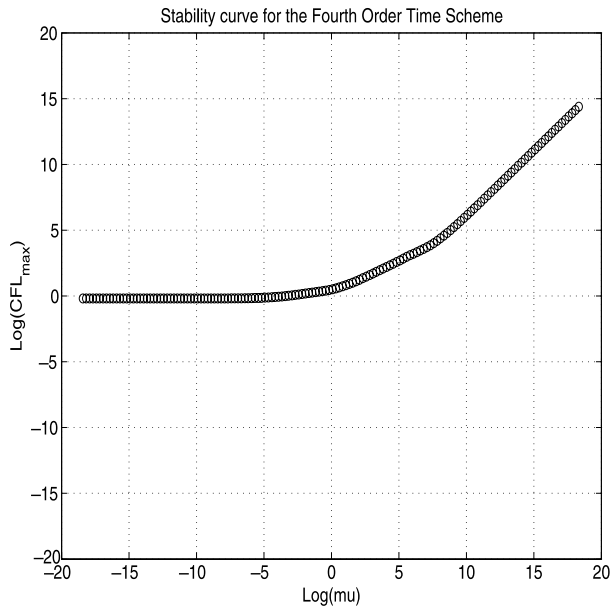
Equivalently,

$$E^2\bar{C}_1^6 + (B^2 - 2ED)\bar{C}_1^4 + (-2AB + D^2)\bar{C}_1^2 + A^2 - F \leq 0. \tag{5.78}$$

Note that A, B, D, E, F depend on the parameter (θ, φ) and also on μ, where the dependence on μ is via $\bar{B}_1$ and the dependence on λ is via $\bar{C}_1$ (see (5.61), (5.11), (5.16)). For a given μ, we find a condition on λ so that (5.78) is satisfied, as follows:

$$\bar{C}_1^2 \leq z(\theta, \varphi, \mu), \quad \text{for all } (\theta, \varphi), \tag{5.79}$$

where $z(\theta, \varphi, \mu)$ is the first positive root of the cubic polynomial $P_{\mu, \theta, \varphi}(z)$ defined by

$$P_{\mu, \theta, \varphi}(z) = E^2 z^3 + (B^2 - 2ED)z^2 + (-2AB + D^2)z + A^2 - F. \tag{5.80}$$

Note that this root exists since $A^2 - F < 0$ for all θ, φ and $P_{\mu, \theta, \varphi}(z) \to +\infty$ when $z \to +\infty$. Since

$$\bar{C}_1^2 \leq \lambda^2 \tilde{D}(\theta, \varphi), \tag{5.81}$$

using (5.79) we find that a sufficient condition for stability is

$$\lambda^2 \leq \min_{\theta, \varphi} \frac{z(\theta, \varphi, \mu)}{\tilde{D}(\theta, \varphi)} := CFL_3^2(\mu). \tag{5.82}$$

In Fig. 2 we display in Log-Log scale the curve

$$\mu \mapsto CFL_3(\mu). \tag{5.83}$$

The graph is computed numerically using, as in Sect. 5.2, a sampling of θ, $\varphi \in [0, 2\pi)$, and of $\mu > 0$.

6 Numerical Results for the Navier-Stokes Equations

6.1 FFT Linear Solver

Recall that the approximation of the Navier-Stokes equation in pure streamfunction form (3.1) is treated implicitly for the diffusive part and explicitly for the convective term. Therefore, at each time-step, we have to solve a set of linear equations of the form

$$(\tilde{\Delta}_h - \kappa \nu \Delta t \tilde{\Delta}_h^2)\psi = g. \tag{6.1}$$

Here κ is a constant, which depends on Δt and on some parameters of the time-stepping scheme. Note that at each time-step the second order time-stepping scheme (4.5) requires two solutions (with different parameters κ) of (6.1), whereas the higher-order time-stepping scheme (4.8) requires three such solutions. The resolution of the linear system is performed by the fast solver described in [9]. It uses the Sine Basis Functions. For the no-slip boundary condition the solver described in [9] incorporates this condition in the algorithm by a capacitance matrix method and the use of the Sherman-Morrison theorem. For the non-homogeneous boundary condition, see Sect. 3.4 in [9]. This solver is of $O(N^2 \text{Log}(N))$ operations, where N is the number of points in any direction. As an example, we note that one resolution of (6.1) for $N = 129$ takes less than 0.05 seconds on a time-step on a 3 GHz PC with 2 GO memory.

6.2 Numerical Accuracy with the Second Order Time-Scheme

In order to verify the spatial fourth order accuracy of the scheme, we performed several numerical tests using the second order time-stepping scheme (4.5). For the convective term we use one of the fourth order approximations (3.25) or (3.42). Since we are interested in the fourth order accuracy in space, we have to restrict the time-step to $\Delta t = Ch^2$, where C is a constant. Note that it is more restrictive than any of the stability conditions derived in Sect. 5.

6.2.1 Case 1

$\psi(x, y, t) = (1 - x^2)^3(1 - y^2)^3 e^{-t}$ on $\Omega = [-1, 1] \times [-1, 1]$. Take

$$f(x, y, t) = \partial_t \Delta \psi + \nabla^\perp \psi \cdot \nabla \Delta \psi - \Delta^2 \psi, \tag{6.2}$$

where $\psi(x, y, t) = (1 - x^2)^3(1 - y^2)^3 e^{-t}$. Our aim is to recover $\psi(x, y, t)$ from $f(x, y, t)$. Thus, we resolve numerically

$$\begin{cases} \partial_t \Delta \psi + \nabla^\perp \psi \cdot \nabla \Delta \psi - \Delta^2 \psi = f(x, y, t), \\ \psi(x, y, 0) = (1 - x^2)^3(1 - y^2)^3, \\ \psi(x, y, t) = 0, \qquad \dfrac{\partial \psi(x, y, t)}{\partial n} = 0, \quad (x, y) \in \partial\Omega. \end{cases} \tag{6.3}$$

In the tables below we present the error e and the relative error, e_r, where

$$e_{l_2} = \|\psi_{\text{comp}} - \psi_{\text{exact}}\|_{l^2}, \qquad e_r = e/\|\psi_{\text{exact}}\|_{l^2}$$

Table 1 Compact scheme for Navier-Stokes with exact solution: $\psi = (1 - x^2)^3(1 - y^2)^3e^{-t}$ on $[-1, 1] \times [-1, 1]$. We present e, the l_2 error for the streamfunction and e_x the max error in the $u = -\partial_y\psi$. The convective term is (3.25)

Mesh	9×9	Rate	17×17	Rate	33×33	Rate	65×65
$t = 0.25\,e$	5.0839(−3)	4.06	3.0510(−4)	4.02	1.8825(−5)	4.00	1.1728(−6)
e_r	9.4884(−3)		5.7414(−4)		3.5443(−5)		2.2081(−6)
e_x	2.6385(−3)	3.89	1.7837(−4)	3.93	1.1662(−5)	3.98	7.3752(−7)
$t = 0.5\,e$	3.2225(−3)	4.00	2.0078(−4)	4.00	1.2536(−5)	4.00	7.8331(−7)
e_r	7.7371(−3)		4.8519(−4)		3.0305(−5)		1.8937(−6)
e_x	3.2290(−3)	4.02	1.9897(−4)	4.00	1.2437(−5)	4.00	7.7747(−7)
$t = 0.75\,e$	2.4880(−3)	4.00	1.5505(−4)	4.00	9.6864(−6)	4.00	6.0537(−7)
e_r	7.6708(−3)		4.8108(−4)		3.0068(−5)		1.8792(−6)
e_x	2.5519(−3)	4.03	1.5723(−4)	4.00	9.8188(−6)	4.00	6.1365(−7)
$t = 1\,e$	1.9373(−3)	4.00	1.2072(−4)	4.00	7.5424(−6)	4.00	4.7138(−7)
e_r	7.6692(−3)		4.8096(−4)		3.0062(−5)		1.8788(−6)
e_x	1.9886(−3)	4.02	1.2255(−4)	4.00	7.6527(−6)	4.00	4.7827(−7)

and

$$e_u = \|u_{\text{comp}} - u_{\text{exact}}\|_{l^2}.$$

Here, ψ_{comp}, u_{comp} and ψ_{exact}, u_{exact} are the computed and the exact streamfunction and x-component of the velocity field, respectively. We represent results for different time-levels and number of mesh points. In Table 1 we present numerical results for the approximation (3.25) of the convective term. We observe clearly that applying our scheme with the convective term (3.25) (the no-leak/periodic case) yields fourth order accuracy for ψ and the gradient of ψ. The results are displayed in Table 1.

In Fig. 3 we display in a Log/Log scale the error in ψ (shown numerically in Table 1) for the four different time levels $t = 0.25, 0.5, 0.75, 1$. It can be clear from Fig. 3 that the slope of the graph is almost constant, which is around four. Table 2 displays the results obtained by the approximation (3.42) (the general boundary conditions case) of the convective term.

6.2.2 Case 2

$\psi = e^{-2x-y}e^{-t}$ on $[0, 1] \times [0, 1]$ In Table 3 we display numerical results for $\psi = e^{-2x-y}e^{-t}$, using the convective term (3.42) (the general boundary condition case).

6.2.3 Case 3

$\psi = (1 - x^2)^3(1 - y^2)^3e^{-t}$ on $[0, 1] \times [0, 1]$. In Table 4 we present numerical results for $\psi = (1 - x^2)^3(1 - y^2)^3e^{-t}$ on $[0, 1] \times [0, 1]$, using the convective term (3.42).

Observe that in all test cases with the second order time-stepping scheme fourth-order accuracy in space and second order accuracy in time are achieved.

Fig. 3 Log(h) ↦
Log($error(h)$). Case 6.2.1,
second-order time-stepping
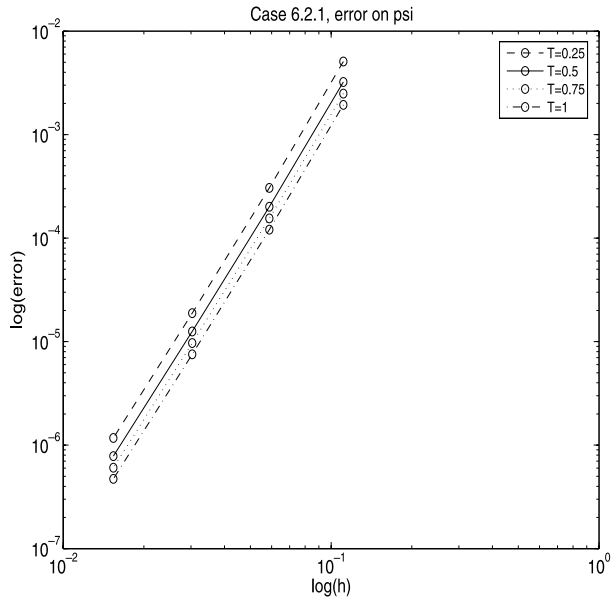scheme, no-leak boundary
condition

Table 2 Compact scheme for Navier-Stokes with exact solution: $\psi = (1 - x^2)^3(1 - y^2)^3 e^{-t}$ on $[-1, 1] \times [-1, 1]$. We present e, the l_2 error for the streamfunction and e_x the max error in the $u = -\partial_y \psi$. The convective term is (3.42)

Mesh	9×9	Rate	17×17	Rate	33×33	Rate	65×65
$t = 0.25\,e$	5.0867(-3)	4.06	3.0525(-4)	4.02	1.8835(-5)	4.00	1.1734(-6)
e_r	9.4936(-3)		5.7441(-4)		3.5460(-5)		2.2092(-6)
e_x	2.6390(-3)	3.89	1.7837(-4)	3.93	1.1670(-5)	3.98	7.3752(-7)
$t = 0.5\,e$	3.2224(-3)	4.00	2.0085(-4)	4.00	1.2541(-5)	4.00	7.8361(-7)
e_r	7.7407(-3)		4.8536(-4)		3.0317(-5)		1.8944(-6)
e_x	3.2285(-3)	4.02	1.9896(-4)	4.00	1.2436(-5)	4.00	7.7745(-7)
$t = 0.75\,e$	2.4887(-3)	4.00	1.5508(-4)	4.00	9.6887(-6)	4.00	6.0551(-7)
e_r	7.6730(-3)		4.8119(-4)		3.0075(-5)		1.8796(-6)
e_x	2.5516(-3)	4.02	1.5723(-4)	4.00	9.8187(-6)	4.00	6.1364(-7)
$t = 1\,e$	1.9376(-3)	4.00	1.2074(-4)	4.00	7.5434(-6)	4.00	4.7145(-7)
e_r	7.6796(-3)		4.8103(-4)		3.0066(-5)		1.8791(-6)
e_x	1.9885(-3)	4.02	1.2255(-4)	4.00	7.6526(-6)	4.00	4.7826(-7)

6.3 Numerical Accuracy with the Higher Order Time-Scheme

6.3.1 Case 1

$\psi(x, y, t) = (1 - x^2)^3(1 - y^2)^3 e^{-t}$ on $[-1, 1] \times [-1, 1]$. Now we consider the time-stepping scheme (4.8) applied to the exact solution $\psi(x, y, t) = (1 - x^2)^3(1 - y^2)^3 e^{-t}$ on $[-1, 1] \times [-1, 1]$. Since the scheme is fourth order accurate in space and almost third order accurate

Table 3 Compact scheme for Navier-Stokes with exact solution: $\psi = e^{-2x-y}e^{-t}$ on $[0, 1] \times [0, 1]$. We present e, the l_2 error for the streamfunction and e_x the max error in the $u = -\partial_y \psi$. The convective term is (3.42) (the general boundary condition case)

Mesh	9×9	Rate	17×17	Rate	33×33	Rate	65×65
$t = 0.25\, e$	8.4636(−7)	3.94	5.5306(−7)	3.97	3.5412(−8)	3.98	2.2491(−10)
e_r	4.1691(−6)		2.4301(−7)		1.4728(−8)		9.1050(−10)
e_x	8.6714(−6)	3.79	6.2534(−5)	3.90	4.1890(−8)	3.93	2.7576(−9)
$t = 0.5\, e$	6.5253(−7)	3.93	4.2671(−8)	3.96	2.7421(−9)	3.98	1.7429(−10)
e_r	4.1272(−6)		2.4126(−7)		1.4644(−8)		9.0600(−10)
e_x	6.6869(−6)	3.79	4.8421(−7)	3.90	3.2522(−8)	3.93	2.1389(−8)
$t = 0.75\, e$	5.0415(−7)	3.93	3.3112(−8)	3.96	2.1259(−9)	3.97	1.3521(−10)
e_r	4.0944(−6)		2.3988(−7)		1.4577(−8)		9.0244(−10)
e_x	5.1672(−6)	3.78	3.7539(−7)	3.87	2.5266(−8)	3.95	1.6605(−9)
$t = 1\, e$	3.9017(−7)	3.93	2.5671(−8)	3.96	1.6494(−9)	3.97	1.0497(−10)
e_r	4.0687(−6)		2.3879(−7)		1.4525(−8)		8.9965(−10)
e_x	3.9952(−6)	3.78	2.9132(−7)	3.89	1.9639(−8)	3.93	1.2900(−9)

Table 4 Compact scheme for the Navier-Stokes with exact solution: $\psi = (1-x^2)^3(1-y^2)^3 e^{-t}$ on $[0, 1] \times [0, 1]$. We present e, the l_2 error for the streamfunction and e_x the max error in the $u = -\partial_y \psi$. The convective term is (3.42)

Mesh	9×9	Rate	17×17	Rate	33×33	Rate	65×65
$t = 0.25\, e$	2.3767(−5)	3.91	1.5792(−7)	3.95	1.0232(−7)	4.03	6.5236(−9)
e_r	1.0958(−4)		6.5463(−6)		4.0380(−7)		2.5141(−8)
e_x	7.2161(−4)	3.91	4.7907(−5)	3.97	3.0612(−6)	3.97	1.9347(−7)
$t = 0.5\, e$	1.8518(−5)	3.91	1.2315(−7)	3.95	7.9827(−8)	3.97	5.0902(−9)
e_r	1.0963(−4)		6.5554(−6)		4.0450(−7)		2.5188(−8)
e_x	5.6231(−4)	3.91	3.7309(−5)	3.97	2.3840(−6)	3.98	1.5067(−7)
$t = 0.75\, e$	1.4425(−5)	3.91	9.5991(−7)	3.95	6.2235(−8)	3.97	3.9688(−9)
e_r	1.0965(−4)		6.5609(−6)		4.0993(−7)		2.5217(−8)
e_x	4.3811(−4)	3.91	2.9055(−5)	3.97	1.8566(−6)	3.98	1.1173(−7)
$t = 1\, e$	1.1236(−5)	3.91	7.5671(−7)	3.95	4.8500(−8)	3.97	3.0930(−9)
e_r	1.0967(−4)		6.3879(−6)		4.0520(−7)		2.5235(−8)
e_x	3.1319(−4)	3.92	2.9132(−5)	3.97	1.4459(−6)	3.98	9.1385(−7)

in time [49], we picked Δt as the minimum between $\Delta t = Ch^{4/3}$ and the value of Δt as restricted in Sect. 5. The results are shown in Table 5.

In Table 6 we present similar results to those in Table 5, but now with the approximation (3.42) for the general boundary conditions case.

Table 5 Compact scheme for the Navier-Stokes equations with exact solution: $\psi = (1 - x^2)^3(1 - y^2)^3 e^{-t}$ on $[-1, 1] \times [-1, 1]$. We present e, the l_2 error for the streamfunction and e_x the max error in the $u = -\partial_y \psi$. Convective term (3.25). Time-stepping scheme (4.8) with $\Delta t = Ch^{4/3}$

Mesh	17×17		33×33	Rate	65×65	Rate	129×129
$t = 0.25\,e$	7.2167(−5)	4.02	4.4322(−6)	3.62	3.5965(−7)	3.29	3.6776(−8)
e_r	1.3562(−4)		8.3286(−6)		6.7714(−7)		6.9129(−8)
e_x	7.5017(−4)	4.08	4.4344(−5)	4.20	2.4146(−6)	4.36	1.1739(−7)
$t = 0.5\,e$	9.4956(−5)	3.80	6.8184(−6)	3.69	5.2714(−7)	3.60	4.3554(−8)
e_r	2.3091(−4)		1.6484(−5)		1.2744(−6)		1.0527(−7)
e_x	4.3941(−4)	4.11	2.5365(−5)	4.24	1.3468(−6)	4.45	6.1584(−8)
$t = 0.75\,e$	1.1601(−4)	3.86	7.9992(−6)	3.80	5.7617(−7)	3.73	4.3400(−8)
e_r	3.6146(−4)		2.4783(−5)		1.7885(−6)		1.3476(−7)
e_x	2.4736(−4)	4.15	1.3973(−5)	4.31	7.0510(−7)	4.62	2.8624(−8)
$t = 1\,e$	1.2156(−4)	3.90	8.1623(−6)	3.85	5.6441(−7)	3.81	4.0340(−8)
e_r	4.8531(−4)		3.2535(−5)		2.2496(−6)		1.6072(−8)
e_x	1.2681(−4)	4.23	6.7792(−6)	4.26	3.5366(−7)	3.86	2.4347(−8)

Table 6 Compact scheme for the Navier-Stokes equations with exact solution: $\psi = (1 - x^2)^3(1 - y^2)^3 e^{-t}$ on $[-1, 1] \times [-1, 1]$. We present e, the l_2 error for the streamfunction and e_x the max error in the $u = -\partial_y \psi$. The convective term is (3.42). Time-stepping scheme (4.8) with $\Delta t = Ch^{4/3}$

Mesh	17×17	Rate	33×33	Rate	65×65	Rate	129×129
$t = 0.25\,e$	7.4854(−5)	3.99	4.6895(−6)	3.63	3.7909(−7)	3.32	3.7958(−8)
e_r	1.4066(−4)		8.8121(−6)		7.1373(−7)		7.1458(−8)
e_x	7.4490(−4)	4.07	4.4217(−5)	4.19	2.4174(−6)	4.35	1.1850(−7)
$t = 0.5\,e$	9.9615(−5)	3.79	7.1931(−6)	3.71	5.5081(−7)	3.61	4.5021(−8)
e_r	2.3984(−4)		1.7390(−5)		1.3316(−6)		1.0882(−7)
e_x	4.3783(−4)	4.15	2.4698(−5)	4.23	1.3166(−6)	4.44	6.7634(−8)
$t = 0.75\,e$	1.2097(−4)	3.86	8.3195(−6)	3.80	5.9586(−7)	3.74	4.4637(−8)
e_r	3.7691(−4)		2.5877(−5)		1.8496(−6)		1.3852(−7)
e_x	2.3823(−4)	4.17	1.3258(−5)	4.30	6.7180(−7)	4.41	3.1705(−8)
$t = 1\,e$	1.2534(−4)	3.90	8.3958(−6)	3.85	5.7918(−7)	3.81	4.1269(−8)
e_r	4.9546(−4)		3.3466(−5)		2.3085(−6)		1.6442(−7)
e_x	1.2362(−4)	4.28	6.3472(−6)	4.02	3.8993(−7)	3.87	2.6737(−8)

6.3.2 Case 2

$\psi = e^{-2x-y}e^{-t}$ on $[0, 1] \times [0, 1]$. Table 7 summarizes the results for $\psi = e^{-2x-y}e^{-t}$ on $[0, 1] \times [0, 1]$, using the scheme (3.42) (general boundary conditions) for the convective term.

Note that for this test case the convergence rates from $N = 17$ to $N = 33$ and from $N = 33$ to $N = 65$ are around 4. However, the convergence rate from $N = 65$ to $N = 129$

Table 7 Compact scheme for the Navier-Stokes equations with exact solution: $\psi = e^{-2x-y}e^{-t}$ on $[0, 1] \times [0, 1]$. We present e, the l_2 error for the streamfunction and e_x the max error in the $u = -\partial_y \psi$. The convective term is (3.42). Time-stepping scheme (4.8) with $\Delta t = Ch^{4/3}$

Mesh	17×17	Rate	33×33	Rate	65×65	Rate	129×129
$t = 0.25\,e$	$5.8771(-8)$	3.99	$3.6392(-9)$	4.00	$2.3074(-10)$	2.38	$4.5343(-11)$
e_r	$2.5875(-7)$		$1.5135(-8)$		$2.0170(-9)$		$1.8113(-10)$
e_x	$8.8547(-7)$	4.06	$5.3189(-8)$	4.06	$3.1913(-9)$	3.11	$3.6950(-10)$
$t = 0.5\,e$	$5.1921(-8)$	4.02	$3.1994(-9)$	4.00	$2.0005(-10)$	2.12	$4.5875(-11)$
e_r	$2.9294(-7)$		$1.7085(-8)$		$1.0397(-9)$		$2.3531(-10)$
e_x	$6.5312(-7)$	4.05	$3.9263(-8)$	4.04	$2.3807(-9)$	2.71	$3.6286(-10)$
$t = 0.75\,e$	$4.0887(-8)$	4.00	$2.5261(-8)$	4.00	$1.5801(-10)$	2.03	$3.8699(-11)$
e_r	$2.9564(-7)$		$1.7321(-8)$		$1.0543(-9)$		$2.5488(-10)$
e_x	$4.7850(-7)$	4.03	$2.9192(-8)$	4.03	$1.7857(-8)$	2.56	$3.0230(-10)$
$t = 1\,e$	$3.1381(-8)$	4.01	$1.9470(-9)$	3.99	$1.2212(-10)$	1.97	$3.1174(-11)$
e_r	$2.9078(-7)$		$1.7142(-8)$		$1.0468(-9)$		$2.6365(-10)$
e_x	$9.2348(-6)$	4.01	$2.1867(-8)$	4.02	$1.3523(-9)$	2.49	$2.4074(-10)$

has been decreased, whereas in the previous two test cases (shown in Tables 5 and 6) the convergence rate is around 4. The reason for the reduced accuracy for $N = 129$ in case 2 is that the errors in the last column of Table 7 are very small, and they actually reach the accuracy of the computer. In the next example we show that the convergence rate is around 4, also at the finest grids level.

6.3.3 Case 3

$\psi(x, y, t) = (1 - x^2)^3(1 - y^2)^3 e^{-t}$ on $[0, 1] \times [0, 1]$. We consider the Spalart et al. scheme applied to the exact solution $\psi(x, y, t) = (1 - x^2)^3(1 - y^2)^3 e^{-t}$ on the square $[0, 1] \times [0, 1]$.

In Fig. 4 we display in a Log/Log scale the error in ψ (shown numerically in Table 8) for the four different time levels $t = 0.25, 0.5, 0.75, 1$. It is clear from Fig. 4 that the slope of the graph is almost constant around four.

6.4 Driven Cavity Test Cases

In this section, we briefly demonstrate the capability of the fourth order accurate scheme (4.8) to compute accurately several classical driven cavity test cases on relatively coarse grids. To assess the spatial accuracy, we limit ourselves to a comparison of the asymptotic states of the classical driven cavity test case for a Reynolds number of $Re = 1000$. This case is well documented in the literature. According to numerous numerical studies, see e.g. [4, 11, 14], there is a unique asymptotic state.

The problem consists of a square $[0, 1] \times [0, 1]$. A horizontal velocity $u = 1$ is specified on the top edge, while both velocity components vanish on all other three sides.

We display the results of $u(1/2, y)$ and $v(x, 1/2)$ as functions of y and x, respectively. These are compared to the results obtained in the classical reference [29]. In Fig. 5, we display on the left the solution, using 33×33 points, subject to the second order scheme presented in [7]. Observe that the reference values (plotted as circles) are not reached at the

Fig. 4 Log(h) $\mapsto$
Log($error(h)$). Case 6.3.3,
Spalart et al. [49] time-stepping
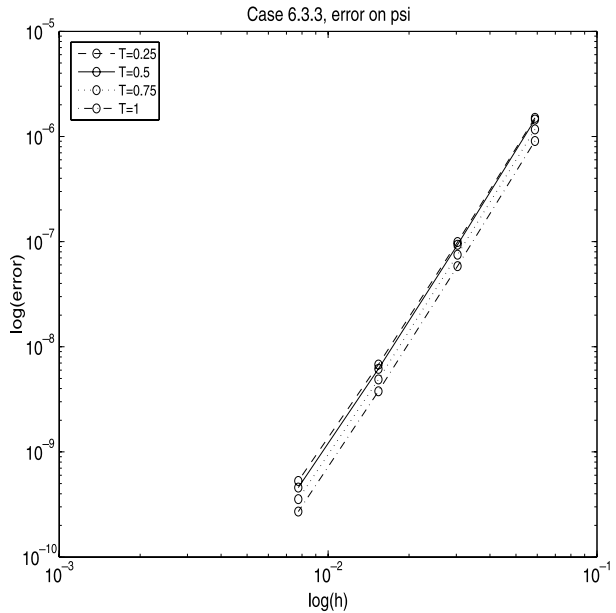scheme, general boundary
conditions

Table 8 Compact scheme for the Navier-Stokes equations with exact solution: $\psi(x, y, t) = (1 - x^2)^3 \times (1 - y^2)^3 e^{-t}$ on $[0, 1] \times [0, 1]$ We present e, the l_2 error for the streamfunction and e_x the max error in the $u = -\partial_y \psi$. The convective term is (3.42). Time-stepping scheme (4.8) with $\Delta t = Ch^{4/3}$

Mesh	17×17	Rate	33×33	Rate	65×65	Rate	129×129
$t = 0.25\, e$	1.5022(−6)	3.92	9.9168(−8)	3.87	6.7763(−9)	3.70	5.2892(−10)
e_r	6.2153(−6)		3.9197(−7)		2.6112(−8)		2.0148(−9)
e_x	4.8052(−5)	3.97	3.0614(−6)	3.98	1.9378(−7)	3.98	1.2254(−8)
$t = 0.5\, e$	1.4466(−6)	3.95	9.3439(−8)	3.92	6.1550(−9)	3.75	4.5764(−10)
e_r	7.7001(−6)		4.7348(−7)		3.0451(−8)		2.2384(−9)
e_x	3.7321(−5)	3.97	2.3877(−6)	3.98	1.5096(−7)	3.98	9.5492(−8)
$t = 0.75\, e$	1.1674(−6)	3.96	7.5132(−8)	3.94	4.8817(−9)	3.78	3.5552(−10)
e_r	7.9635(−6)		4.8884(−7)		3.1027(−8)		2.2329(−9)
e_x	2.9106(−5)	3.97	1.8592(−6)	3.98	1.1175(−7)	3.91	7.4402(−9)
$t = 1\, e$	9.0495(−7)	3.96	5.8434(−8)	3.95	3.7702(−9)	3.80	2.7092(−10)
e_r	7.9423(−6)		4.8819(−7)		3.0765(−8)		2.1849(−9)
e_x	2.2612(−5)	3.97	1.4477(−6)	3.98	9.1540(−7)	3.98	5.7964(−9)

steady-state. On the right we display the solution subject to the fourth order scheme (4.8), using the same number of points. It agrees much better with the reference values. Table 9 contains the locations and values of the maximum-minimum of the streamfunction.

Figure 6 and Table 10 document the same computation with 65×65 points. The agreement with reference solutions in [29] and [14] is quite good. The results with the fourth order scheme are slightly better than those obtained with the second order scheme. We list some
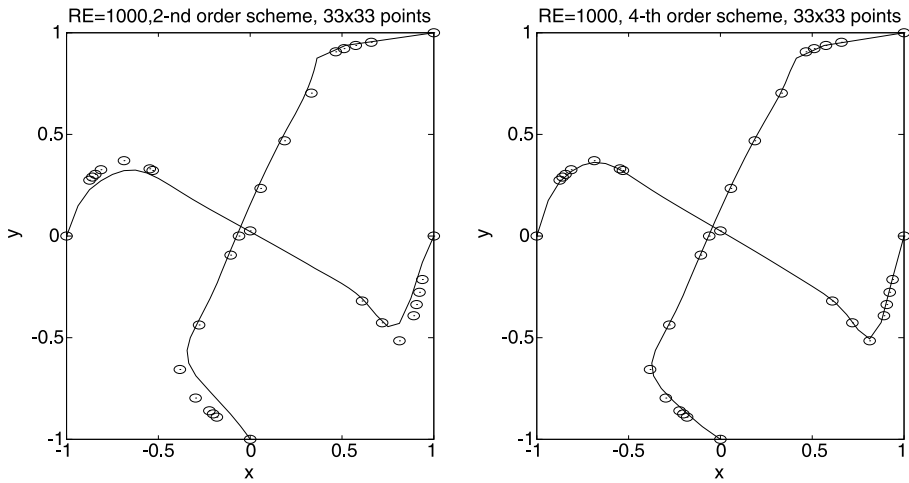
Fig. 5 Driven cavity for Re = 1000: velocity components. Computations are performed with $N = 33$. The second order scheme is on the *left*, and the fourth order scheme on the *right*. The reference results of [29] are plotted with *circles*
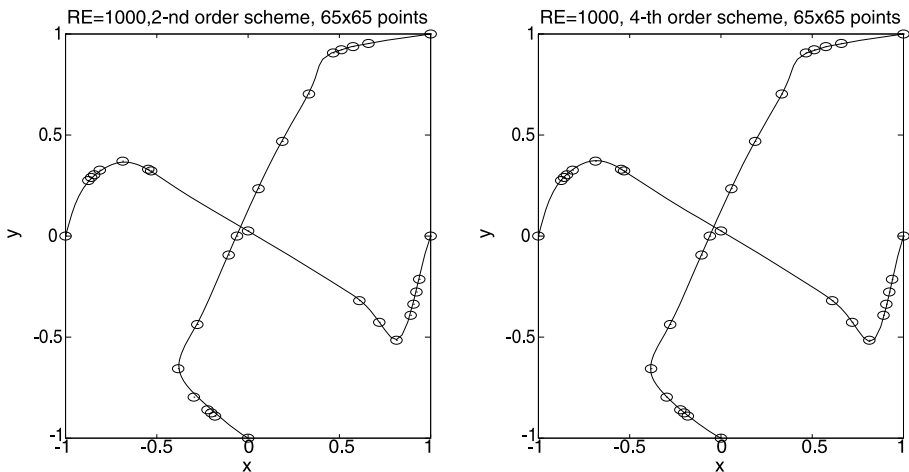

Fig. 6 Driven cavity for Re = 1000: velocity components. Computations are done with $N = 65$. The second order scheme is on the *left*, and the fourth order scheme on the *right*. The reference results of [29] are plotted with *circles*

details concerning the computation using the fourth order scheme with 65×65 points: 8000 time-iterations are performed with a time step $\Delta t = 1/60 \simeq 0.01660$. The physical time reached is $T = 133$ with a residual on the streamfunction of $\mathrm{res}(\psi) = 1.65(-08)$. The CPU per time-step is 0.09375 seconds comprising three biharmonic resolutions per time-step, see (4.8). The global CPU time of the computation is 750 seconds, which demonstrates the efficiency of the fast solver for the biharmonic problem. The computations are performed on a simple Laptop (2.40 GHz, 3GO memory). We refer to [7] for results with the second order scheme where more points are used.

Table 9 Streamfunction formulation: compact scheme for the driven cavity problem, Re = 1000, 33 × 33 points

	2-nd order, $N = 32$	4-th order, $N = 32$	Ghia et al. [29], $N = 128$	Bruneau and Saad [14], $N = 1024$
max ψ	0.10535	0.11541	0.117929	0.11892
$(\bar{x}, \bar{y})$	(0.53125, 0.59375)	(0.53125, 0.56250)	(0.5313, 0.5625)	(0.53125, 0.56543)
min ψ	−0.0016497	−0.0016875	−0.0017510	−0.0017292

Table 10 Streamfunction formulation: compact scheme for the driven cavity problem, Re = 1000, 65 × 65 points

	2-nd order, $N = 64$	4-th order, $N = 64$	Ghia et al. [29], $N = 128$	Bruneau and Saad [14], $N = 1024$
max ψ	0.116032	0.118033	0.117929	0.11892
$(\bar{x}, \bar{y})$	(0.53125, 0.56250)	(0.53125, 0.56250)	(0.5313, 0.5625)	(0.53125, 0.56543)
min ψ	−0.0017083	−0.0017067	−0.0017510	−0.0017292

7 Conclusion

This work presents the design of a fourth order accurate scheme for the Navier-Stokes equation in pure-streamfunction formulation in the general framework of [7]. In particular we show how to approximate the non-linear convective term to fourth order. We considered two types of time-stepping schemes . The first one is second order and the second is of higher order. For the first scheme, we obtained stability conditions. An investigation of the fourth order Runge-Kutta scheme with an explicit treatment of the diffusive term and convective terms is underway.

References

1. Altas, I., Dym, J., Gupta, M.M., P Manohar, R.: Mutigrid solution of automatically generated high-order discretizations for the biharmonic equation. SIAM J. Sci. Comput. **19**, 1575–1585 (1998)
2. Ascher, U.M., Ruuth, S.J., Wetton, T.R.: Implicit-explicit methods for time-dependent partial differential equations. SIAM J. Numer. Anal. **32**, 797–823 (1995)
3. Ascher, U.M., Ruuth, S.J., Spiteri, R.J.: Implicit-explicit Runge-Kutta methods for time-dependent partial differential equations. Appl. Numer. Math. **25**(2–3), 151–167 (1997)
4. Auteri, F., Parolini, N., Quartapelle, L.: Numerical investigation on the stability of the singular driven cavity flow. J. Comput. Phys. **183**, 1–25 (2002)
5. Bell, J.B., Colella, P., Glaz, H.M.: A second-order projection method for the incompressible Navier-Stokes equations. J. Comput. Phys. **85**, 257–283 (1989)
6. Ben-Artzi, M., Fishelov, D., Trachtenberg, S.: Vorticity dynamics and numerical resolution of Navier-Stokes equations. Math. Model. Numer. Anal. **35**(2), 313–330 (2001)
7. Ben-Artzi, M., Croisille, J.-P., Fishelov, D., Trachtenberg, S.: A pure-compact scheme for the stream-function formulation of Navier-Stokes equations. J. Comput. Phys. **205**(2), 640–664 (2005)

8. Ben-Artzi, M., Croisille, J.-P., Fishelov, D.: Convergence of a compact scheme for the pure streamfunction formulation of the unsteady Navier-Stokes system. SIAM J. Numer. Anal. **44**(5), 1997–2024 (2006)

9. Ben-Artzi, M., Croisille, J.-P., Fishelov, D.: A fast direct solver for the biharmonic problem in a rectangular grid. SIAM J. Sci. Comput. **31**(1), 303–333 (2008)

10. Ben-Artzi, M., Chorev, I., Croisille, J.-P., Fishelov, D.: A compact difference scheme for the biharmonic equation in planar irregular domains. SIAM J. Numer. Anal. (2009)

11. Botella, O., Peyret, R.: Benchmark spectral results on the lid-driven cavity flow. Comput. Fluids **27**, 421–433 (1998)

12. Brown, D.L., Cortez, R., Minion, M.L.: Accurate projection methods for the incompressible Navier-Stokes equations. J. Comput. Phys. **168**, 464–499 (2001)

13. Brüger, A., Gustafsson, B., Lötstedt, P., Nilsson, J.: High order accurate solution of the incompressible Navier-Stokes equations. J. Comput. Phys. **203**, 49–71 (2005)

14. Bruneau, C.-H., Saad, M.: The 2d lid-driven cavity revisited. Comput. Fluids **35**, 326–348 (2006)

15. Bubnovitch, V.I., Rosas, C., Moraga, N.O.: A stream function implicit difference scheme for 2d incompressible flows of Newtonian fluids. Intl. J. Numer. Methods Eng. **53**, 2163–2184 (2002)

16. Canuto, C., Hussaini, M.Y., Quarteroni, A., Zang, T.A.: Spectral Methods Evolution to Complex Geometries and Applications to Fluid Dynamics. Series in Scientific Computation. Springer, Berlin (2007)

17. Carey, G.F., Spotz, W.F.: High-order compact scheme for the stream-function vorticity equations. Intl. J. Numer. Methods Eng. **38**, 3497–3512 (1995)

18. Carey, G.F., Spotz, W.F.: Extension of high-order compact schemes to time dependent problems. Numer. Methods Partial Differ. Equ. **17**(6), 657–672 (2001)

19. Carpenter, M.H., Gottlieb, D., Abarbanel, S.: The stability of numerical boundary treatments for compact high-order schemes finite difference schemes. J. Comput. Phys. **108**, 272–295 (1993)

20. Cayco, M.E., Nicolaides, R.A.: Finite element technique for optimal pressure recovery from stream function formulation of viscous flows. Math. Comput. **46**, 371–377 (1986)

21. Chorin, A.J.: Numerical solution of the Navier-Stokes equations. Math. Comput. **22**, 745–762 (1968)

22. Chorin, A.J.: Numerical study of slightly viscous flow. J. Fluid Mech. **57**, 785–796 (1973)

23. Chorin, A.J.: Vortex sheet approximation of boundary layers. J. Comput. Phys. **27**, 428–442 (1978)

24. Chorin, A.J.: Vortex models and boundary layer instability. SIAM J. Sci. Stat. Comput. **1**(1), 1–21 (1980)

25. Dean, E.J., Glowinski, R., Pironneau, O.: Iterative solution of the stream function-vorticity formulation of the Stokes problem, application to the numerical simulation of incompressible viscous flow. Comput. Methods Appl. Mech. Eng. **87**, 117–155 (1991)

26. E, W., Liu, J.-G.: Vorticity boundary condition and related issues for finite difference scheme. J. Comput. Phys. **124**, 368–382 (1996)

27. E, W., Liu, J.-G.: Essentially compact schemes for unsteady viscous incompressible flows. J. Comput. Phys. **126**, 122–138 (1996)

28. Fishelov, D., Ben-Artzi, M., Croisille, J.-P.: A compact scheme for the streamfunction formulation of Navier-Stokes equation. In: Computational Science and Its Applications—ICCSA 2003, Part I. Lecture Notes in Computer Science, vol. 2667, pp. 809–817. Springer, Berlin (2003)

29. Ghia, U., Ghia, K.N., Shin, C.T.: High-Re solutions for incompressible flow using the Navier-Stokes equations and a multigrid method. J. Comput. Phys. **48**, 387–411 (1982)

30. Goodrich, J.W.: An unsteady time-asymptotic flow in the square driven cavity. Technical report tech. mem. 103141, NASA (1990)

31. Goodrich, J.W., Soh, W.Y.: Time-dependent viscous incompressible Navier-Stokes equations: the finite difference Galerkin formulation and streamfunction algorithms. J. Comput. Phys. **84**(1), 207–241 (1989)

32. Goodrich, J.W., Gustafson, K., Halasi, K.: Hopf bifurcation in the driven cavity. J. Comput. Phys. **90**, 219–261 (1990)

33. Gresho, P.M.: Incompressible fluid dynamics: some fundamental formulation issues. Annu. Rev. Fluid Mech. **23**, 413–453 (1991)

34. Gupta, M.M., Kalita, J.C.: A new paradigm for solving Navier-Stokes equations: streamfunction-velocity formulation. J. Comput. Phys. **207**(2), 52–68 (2005)

35. Gupta, M.M., Manohar, R.P., Stephenson, J.W.: Single cell high order scheme for the convection-diffusion equation with variable coefficients. Intl. J. Numer. Methods Fluids **4**, 641–651 (1984)

36. Gustafson, K., Halasi, K.: Cavity flow dynamics at higher Reynolds number and higher aspect ratio. J. Comput. Phys. **70**(2), 271–283 (1987)

37. Hestaven, Y., Gottlieb, S., Gottlieb, D.: Spectral Methods for Time-Dependent Problems. Cambridge Monographs on Applied and Computational Mathematics. Cambridge University Press, Cambridge (2007)

38. Hou, T.Y., Wetton, B.T.R.: Stable fourth order stream-function methods for incompressible flows with boundaries. J. Comput. Math. **27**, 441–458 (2009)

39. Kobayashi, M.H., Pereira, J.M.C.: A computational streamfunction method for the two-dimensional incompressible flows. Intl. J. Numer. Methods Eng. **62**, 1950–1981 (2005)
40. Kosma, Z.: A computing laminar incompressible flows over a backward-facing step using Newton iterations. Mech. Res. Commun. **27**, 235–240 (2000)
41. Kupferman, R.: A central-difference scheme for a pure streamfunction formulation of incompressible viscous flow. SIAM J. Sci. Comput. **23**(1), 1–18 (2001)
42. Lele, S.K.: Compact finite-difference schemes with spectral-like resolution. J. Comput. Phys. **103**, 16–42 (1992)
43. Li, M., Tang, T.: A compact fourth-order finite difference scheme for unsteady viscous incompressible flows. J. Sci. Comput. **16**(1), 29–45 (2001)
44. Lomtev, I., Karniadakis, G.: A discontinuous Galerkin method for the Navier-Stokes equations. Intl. J. Numer. Methods Fluids **29**(5), 587–603 (1999)
45. Orszag, S.A., Israeli, M.: Numerical simulation of viscous incompressible flows. Annu. Rev. Fluid Mech. **6**, 281–318 (1974) (Van Dyke, M., Vincenti, W.A., Wehausen, J.V. (eds.))
46. Quartapelle, L.: Numerical Solution of the Incompressible Navier-Stokes Equations. Birkhäuser, Basel (1993)
47. Quartapelle, L., Valz-Gris, F.: Projection conditions on the vorticity in viscous incompressible flows. Intl. J. Numer. Methods Fluids **1**, 129–144 (1981)
48. Schreiber, R., Keller, H.B.: Driven cavity flows by efficient numerical techniques. J. Comput. Phys. **49**, 310–333 (1983)
49. Spalart, P.R., Moser, R.D., Rogers, M.M.: Spectral methods for the Navier-Stokes equations with one infinite and two periodic directions. J. Comput. Phys. **96**, 297–324 (1991)
50. Stephenson, J.W.: Single cell discretizations of order two and four for biharmonic problems. J. Comput. Phys. **55**, 65–80 (1984)
51. Strikwerda, J.: Finite Difference Schemes and Partial Differential Equations. Wadsworth and Brooks/Cole (1989)
52. Temam, R.: Sur l'approximation de la solution des equations de Navier-Stokes par la methode des pas fractionnaires II. Arch. Ration. Mech. Anal. **33**, 377–385 (1969)
53. Tezduyar, T.E., Liou, J., Ganjoo, D.K., Behr, M.: Solution techniques for the vorticity-streamfunction formulation of the two-dimensional unsteady incompressible flows. Intl. J. Numer. Methods Fluids **11**, 515–539 (1990)
54. Yuan, L., Shu, C.-W.: Discontinuous Galerkin method based on non-polynomial approximation spaces. J. Comput. Phys. **218**(1), 295–323 (2006)